ISSN 0097-3157

PROCEEDINGS OF THE ACADEMY OF NATURAL SCIENCES OF PHILADELPHIA 156: 1-25 JUNE 2007

Redescription of *Orthosternarchus tamandua* (Boulenger, 1898) (Gymnotiformes, Apteronotidae), with reviews of its ecology, electric organ discharges, external morphology, osteology, and phylogenetic affinities

Eric J. Hilton
Geology Department, Field Museum, 1400 South Lake Shore Drive, Chicago IL, 60605. Email: ehilton@fieldmuseum.org

Cristina Cox Fernandes
Instituto Nacional de Pesquisas da Amazônia, C. P. 478, Manaus, Brazil and Biology Department, Morrill Science Center, University of Massachusetts, Amherst MA, 01003, USA, Email: ccf@inpa.gov.br and cristina@bio.umass.edu

John P. Sullivan and John G. Lundberg
Department of Ichthyology, Academy of Natural Sciences, 1900 Benjamin Franklin Parkway, Philadelphia PA, 19103, USA. Email: sullivan@acnatsci.org (JPS); lundberg@acnatsci.org (JGL)

Ricardo Campos-da-Paz
Departamento de Ecologia e Recursos Marinhos, Escola de Ciências Biológicas, Centro de Ciências Biológicas e da Saúde, Universidade Federal do Estado do Rio de Janeiro, Av. Pasteur, 458/sala 408, Urca - Rio de Janeiro, 22290-240, Brazil. Email: rcpaz@sdl.microlink.com.br

ABSTRACT.—In this paper, we redescribe the apteronotid fish *Orthosternarchus tamandua*, the only species of its genus. Historically, *O. tamandua* was rare in collections and only limited anatomical data was available for this species. However, numerous specimens have become available recently as a result of deep-water trawls in the main channel of the Amazon River, thereby making this redescription possible. In addition to describing the external anatomy and osteology of *O. tamandua*, we present data on their electronic organ discharges (EODs) recorded at time of capture, and review what is known of its distribution and ecology. We describe and illustrate the osteology of *O. tamandua*, and in doing so, clarify many aspects of its skeleton. For instance, contrary to previous reports, *O. tamandua* does possess a lateral ethmoid, although it is exceptionally small. We conclude by discussing the EODs of *O. tamandua* in comparison to those of other apteronotids and the anatomical characters used in the support of phylogenetic hypotheses of the genus within the family Apteronotidae.

INTRODUCTION

In 1898, Boulenger described the South American electric knifefish species *Sternarchus tamandua*, which he characterized as having its "snout produced into a long, nearly straight tube, the length of which equals 4 times its depth" (Boulenger, 1898: 427). This description was based on a single individual sent to him by J. Bach (J. Black according to the specimen label of the holotype) from the Rio Juruá of Brazil. Eigenmann and Ward (1905: 165) placed this species in the genus *Sternarchorhamphus*, which was considered to be "intermediate between *Sternarchus* and *Sternarchorhynchus*, having the long snout of the latter and the mouth in size approaching the former." These authors also noted that "this species may represent a genus distinct from *Sternarchorhamphus* as here understood." In his classic review of gymnotiform fishes, Ellis (1913) quoted Boulenger's diagnosis of this species in its entirety and created for it a new monotypic genus, *Orthosternarchus*. Ellis (1913:144) distinguished *Orthosternarchus* from other apteronotids "by the long dorsal thong which has its origin above or slightly behind the pectorals, by the long, straight, tubular snout and by the minute eyes and very short gape." Ellis (1913:pl. 15) considered *Orthosternarchus* to be closely related to the genus *Sternarchorhamphus*, a hypothesis that has been corroborated by recent phylogenetic analysis of the Gymnotiformes (e.g., Alves-Gomes, 1995; Albert, 2001; Triques, 2005).

Orthosternarchus tamandua used to be rare in collections. This species is distributed in the Amazon River drainage, and about 120 specimens were collected with trawls during the Calhamazon project (e.g., see Cox Fernandes et al., 2004; Fig. 1C, D). In this paper, we provide a review of the morphology and biology of *O. tamandua*, including the first description of their electric organ discharges (EODs). We also describe its skeletal anatomy based on newly prepared cleared and stained specimens.

MATERIALS AND METHODS

Specimens.— Most specimens of *O. tamandua* examined in this study, totaling 65 individuals (Appendix 1), were collected as part of the Calhamazon Project between the years 1992 and 1996. The Calhamazon specimens were captured in the deep main channels along more than 2,000 km of the mainstem and tributaries

of the Solimões-Amazon River in Brazil (e.g., Cox Fernandes et al., 2004). Specimens examined ranged in size from 96 to 397 mm TL. Institutional abbreviations follow Leviton et al. (1985).

Electric organ discharges.— Electric organ discharges (EODs) of 12 specimens of *O. tamandua* were recorded, along with those of other gymnotiform species, aboard the river boat *Almirante Guimarães* between 25 October and 14 December 1993. Within one to four hours of its capture, each fish was transferred from a holding tank to a 21 cm x 47 cm x 27 cm plastic cooler containing water from the capture area at the ambient temperature (26.6°C to 29.3°C). Silver/silver-chloride electrodes were positioned at the ends of the container and a ground electrode in the center. The fish was held in place between the electrodes (always facing the positive electrode) inside a nylon mesh sleeve and allowed to acclimate for at least five minutes before being recorded. The signal was amplified with a CWE Corporation bio-amplifier with filters set to 0.1 Hz to 50,000 Hz and low gain. We used a Tektronix 222 portable digital oscilloscope to digitize waveforms at 50 to 500 kHz (8 bit accuracy, 512 points), which were downloaded to a laptop computer. The software package SuperScope II by GW Instruments was used to display and take measurements from these records. EOD records of *O. tamandua* were compared with EODs of the 26 other apteronotid gymnotiform species (minimum estimate) recorded during this project, as well as published apteronotid EODs available in the literature.

Specimens used for recordings were vouchered with individual identification tags and preserved in 10% phosphate buffered formalin. Museum/field numbers and size in millimeters recorded are as follows (organized by river in which collected): Rio Purus: ANSP 187039 (225 mm TL), ANSP 187045 (length not recorded), ANSP 187046 (260 mm TL), ANSP 187047 (285 mm TL); Rio Solimões: ANSP 187042 (345 mm TL); Rio Juruá: OTO-23/2 (uncatalogued; length not recorded); Rio Jutaí: JGL-69/1 (uncatalogued; 120 mm TL), ANSP 187041 (435 mm TL); Rio Içа (lower Putumayo): ANSP 187044 (380 mm TL), ANSP 187036 (405 mm TL), Rio Negro: ANSP 187029 (385 mm TL), ANSP 187030 (280 mm TL).

Anatomical studies.— Twenty-one alcohol-stored specimens examined in this study were x-rayed at the USNM using a Kevex-Varian digital x-ray system and a subset of these were used to collect some meristic data. Four specimens were cleared and stained for bone and cartilage using a protocol based on that of Dingerkus and Uhler (1977). Cleared and stained specimens were examined using binocular dissecting microscopes with substage illumination and camera lucida attachments. Photographs were taken using a Nikon COOLPIX 8700 digital camera using its built in lens or attached to a dissecting microscope using a MM99 Universal Microscope Adapter (Martin Microscope Company, Easley, South Carolina). Final line drawings were rendered electronically using Adobe Illustrator software based on camera lucida sketches.

Morphometric data were collected for 47 individuals. The following 23 measurements were taken point to point with digital calipers to the nearest 0.01 mm: 1, total length, from the tip of the snout to end of caudal fin (TL); 2, anal fin length (AFL); 3, pre-dorsal thong length, from the tip of the snout to the origin of the anterior point on base of dorsal thong (LOD); 4, pre-anus length, from the tip of the snout to the anus and urogenital papilla; 5, head length, distance from the tip of the upper jaw to bony posterior margin of the opercle (H); 6, mouth length, distance from the tip of the mandible to rictus (point where the tissue of upper and lower jaws meet) (M); 7, from anterior edge of right eye to the right pectoral-fin origin; 8, from anterior edge of left eye to the left pectoral-fin origin; 9, from the tip of upper jaw to anterior edge of right eye; 10, from the tip of the upper jaw to anterior edge of left eye; 11, depth at posterior end of the abdominal cavity (AB); 12, maximum depth of body (BD); 13, head depth at the occiput (at tip of supraoccipital spine) (HD); 14, right eye diameter; 15, left eye diameter; 16, distance between middle of the anterior and middle of posterior nares (ID); 17, from the tip of the snout to the middle of anterior naris (N); 18, from the tip of the snout to the middle of posterior naris; 19, from the anterior edge of right eye to the middle of right posterior naris; 20, from the anterior edge of left eye to the middle of left posterior naris; 21, from the anterior edge of right eye to the middle of right anterior naris; 22, from the anterior edge of left eye to the middle of left anterior naris; and 23, length from tip of snout to the 100th anal fin ray (L100). Some of these measurements were described and illustrated in Lundberg et al. (1996) and Cox Fernandes (1998).

Vertebral counts for 21 individuals were divided into abdominal and caudal vertebrae and were made from the x-rays. Abdominal vertebrae counts do not include the anteriormost four centra, which comprise the Weberian apparatus, but rather started with the anteriormost centrum with a full neural spine (c5) and ended at the centra directly above the proximal tip of the posteroventral abdominal bone (= displaced hemal spine of Albert, 2001); caudal vertebrae include all more posterior vertebrae (specimens with obviously broken tails were not included in counts). This landmark was chosen as the division between the two regions because it could be reliably seen on the x-rays and roughly corresponds to the centrum with the first hemal spine, which is often slender and missed on x-rays. Our counts of vertebrae and anal fin rays excluded specimens that had broken tails but included those with regenerated tails, so our counts of caudal vertebrae should be regarded as minimum counts.

We noticed variation in the position of the urogenital papilla, even in specimens of similar sizes. To graphically visualize this, we plotted HL (measurement 5) against the distance from the snout to the urogenital papilla (measurement 4).

To quantify asymmetry in the position of the eyes we used measurements 7-10, 14, 15, and 19-22. Random deviations from symmetry in bilaterally symmetrical traits are referred to as fluctuating asymmetry. To determine if fluctuating asymmetry occurs in the position of the eyes we compared the distribution of right-minus-left character values to a normal distribution with a mean of zero asymmetry (Palmer and Strobeck, 1986; Moller and Swaddle, 1997). Asymmetry is calculated as the difference between the values of the measurements from the left and right sides. Frequency distributions of measurements were then evaluated for deviation against a normal distribution with means values of zero with the Kolmogorov-Smirnov tests. The left-minus-right values were then transformed to numerical values (=

absolute fluctuating asymmetry; Moller and Swaddle, 1997). We plotted asymmetric values versus two variables: 1, types of water in which individuals were collected; and 2, sex.

To explore variation in morphometric features between sexes and between different areas, all 23 measurements were analyzed with Principal Component Analysis on a covariance matrix as described in detail in Cox Fernandes (1998) and Cox Fernandes et al. (2002). In this analysis we included only those specimens that could be sexed based on visual examination of gonads.

SYSTEMATIC DESCRIPTION OF ORTHOSTERNARCHUS TAMANDUA

Apteronotidae Jordan, 1923
Orthosternarchus Ellis, 1913
Orthosternarchus tamandua (Boulenger, 1898)
Figs. 1-3, 7, 9-19, 20A

Sternarchus tamandua Boulenger, 1898: 427; plate 42 (reproduced here as Fig. 2).
Sternarchorhamphus tamandua (Boulenger, 1898); Eigenmann and Ward, 1905: 166.
Orthosternarchus tamandua (Boulenger, 1898); Ellis, 1913: 144; Mago-Leccia, 1994: 31; Albert and Campos-da-Paz, 1998: 429; Albert, 2001: 73.

Holotype.— BMNH 1897.12.1.208 (Fig. 3); 425 mm TL with regenerated tail. Rio Juruá, Amazonas, Brazil (exact locality unknown).

Etymology.— A combination of: *orthos*, straight (Gr.), likely in reference to the straight tubular snout; *sternon*, chest (Gr.), and *archos*, rectum (Gr.), in reference to the anterior position of the urogenital opening in gymnotiform fishes; also a genus of Gymnotiformes and a common suffix for genera in this group of fishes; *tamadu'á*, the anteater (Tupi), likely in reference to its elongate snout. Word derivations adapted from Jaeger (1978) and Ferreira (1986).

Amended diagnosis.— An apteronotid gymnotiform that differs from all other members of the family by the combination of the following characters: long snout tubular and tapers evenly; eye greatly reduced, position often bilaterally asymmetrical; dorsal thong originates far anteriorly, close to posterior margin of skull; two branchiostegals, anterior one slender, posterior one broad and flat; subopercle greatly expanded; filamentous intermuscular ossifications associated with certain muscles of the head (*m. levator operculi*, *m. dilatator operculi*, *m. adductor mandibulae*, and *m. sternohyoideus*); endopterygoid process absent; dorsal margin of opercle concave; posttemporal and supracleithrum separate; mesocoracoid ossified. A monotypic genus.

Distribution and habitat.— *Orthosternarchus tamandua* is limited to the Amazon River basin; known localities from which it has been collected are indicated in Figure 4. *Orthosternarchus tamandua* appears to be a relatively rare species of apteronotid fish. During the Calhamazon project only about 120 specimens of *O. tamandua* were collected, in contrast to more than one thousand specimens of *Sternarchorhamphus mulleri*, a closely related species of similar size, as well as thousands of other electric fishes of various species (Cox Fernandes 1999, Cox Fernandes et al. 2004). Also, in the on-going Catalão project (INPA) more than 300 seine collections have been made (approximately one sampling per month since 1999) in the floodplain channels, at the edges of the river, and in small lakes near Catalão Island. Although more than 30 species of Gymnotiformes have been captured in these areas, not a single specimen of *O. tamandua* has been found.

In the Calhamazon project, *O. tamandua* was caught most often at depths between 6 - 10 meters, but occasionally in less than five meters or between 10—20 meters; it was never collected at depths greater than 20 meters. We collected *O. tamandua* in both white water and black water rivers (sensu Sioli, 1975), and they were most abundant in the Rio Negro and Rio Purus, which are black and white water rivers, respectively. Other studies in the Amazon have collected few specimens of *O. tamandua*. Barletta (1995) collected just four individuals in many trawl samples taken over two years at the confluence of the Rio Solimões and Rio Negro in less than 10 meters of water. Garcia (1995) collected two specimens in 20 trawls of Lake Prato, Anavilhanas (Rio Negro). Thomé de Souza (1999) collected seven specimens in about 35 trawlings on Rio Negro during the strong dry season of September 1997 to February 1998, between 7 and 15 m deep.

ELECTRIC ORGAN DISCHARGES

The EOD of *O. tamandua* can be distinguished from those of all other apteronotid species examined by a very slow repetition rate (mean 530 Hz, range 452 to 605 Hz) in combination with a characteristic monophasic head-negative waveform (Fig. 5a, b). The mean EOD repetition rate of *O. tamandua* is more than eight standard deviations slower than that of any other apteronotid species recorded on the 1993 Calhamazon Expedition and falls within the range more typical of the sternopygid wave gymnotiforms belonging to the genera *Eigenmannia* and *Rhabdolichops*. The waveform consists of a head-negative spike followed by a flat, or nearly flat, head-positive plateau. The leading edge of the negative-going phase is symmetrical with the trailing edge (Fig. 5a) or occasionally exhibits a slight infection in the positive direction (Fig. 5b). This waveform differs from that of most other apteronotid gymnotiforms, which exhibit distinct peaks in both negative and positive directions (e.g. that of *Sternarchorhynchus oxyrhynchus*, Fig. 5d). As in sternopygid gymnotiforms that produce "wave" or "tone" –type EODs from monophasic head-positive discharges, spike-to-spike latency is invariant and similar in duration to the spikes themselves, producing a quasi-sinusoidal EOD. In *O. tamandua*, eight or nine harmonics appear above the –40 dB attenuation level relative to the fundamental frequency (Fig. 5a, b). In our small sample, we observed no relationship between body size or sex and EOD frequency or waveform. The only other adult apteronotid known to have a similar EOD waveform is *Sternarchorhamphus muelleri* (Fig. 5c). However, the EODs of all six *S. muelleri* individuals recorded on the 1993 Calhamazon expedition have significantly faster repetition rates (mean = 937 Hz, range 905 to 986 Hz) than that of *O. tamandua*.

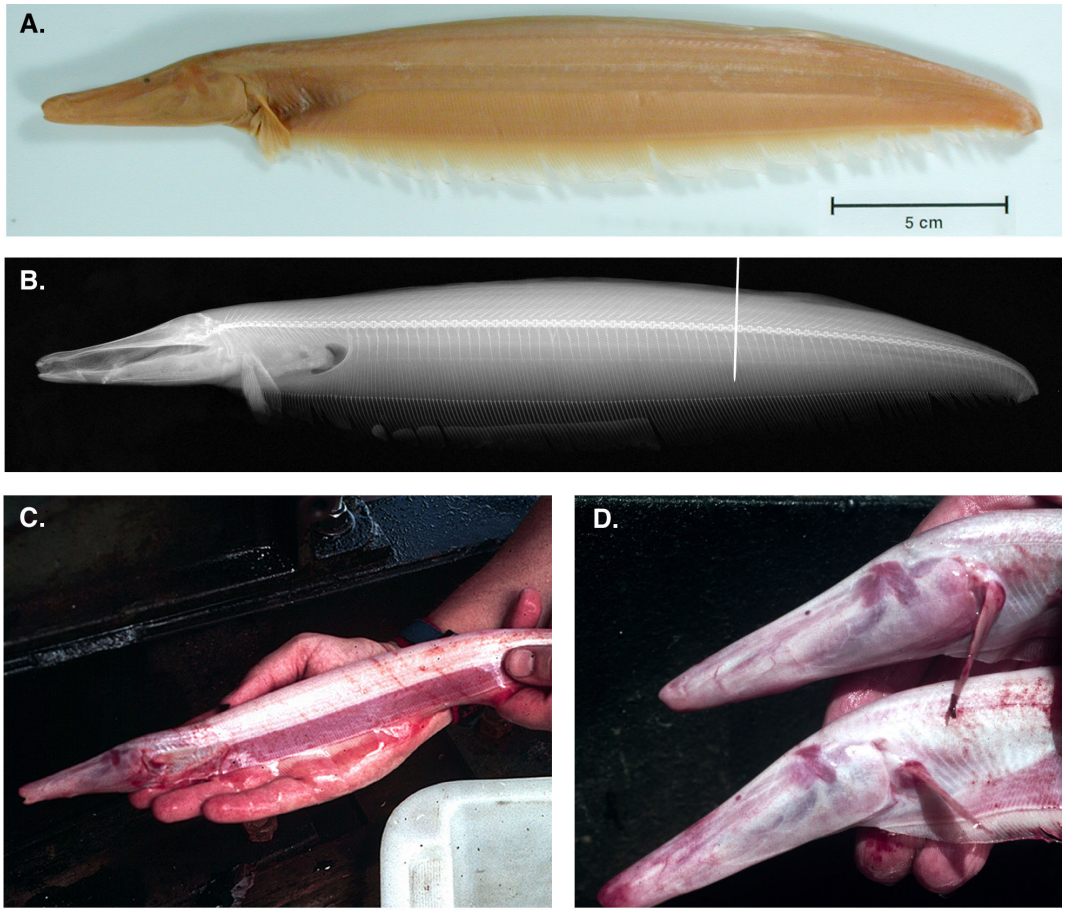

Fig. 1. (A) Photograph and (B) radiograph of whole alcohol-preserved specimen of *Orthosternarchus tamandua* in lateral view (ANSP 187025). (C, D) Recently netted specimens collected during the Calhamazon project.

EXTERNAL MORPHOLOGY AND MORPHOMETRICS

Summaries of the morphometric data of the body measurements we took for *O. tamandua* are presented in Table 1. We found no indication of sexual dimorphism in this species, and no obvious geographic variation was found among individuals collected from the Rio Purus and Rio Negro, which were the two localities from which we had the most specimens. The electroreceptive dorsal thong of *O. tamandua* inserts very far forward on the body, just posterior to the head. This is much further anterior than in other apteronotids (Franchina and Hopkins, 1996) and has been regarded as diagnostic of the genus.

At about 55 mm head length, the position of the urogenital papilla continues its slightly positive allometric growth in some individuals, whereas in others the urogenital papilla is situated behind the mouth (Fig. 6).

Measurements of the head region of *O. tamandua* are summarized in Table 2. The position of the eye is asymmetrical in *O. tamandua* (Fig. 7; also see Fig. 2). Except for the eye diameter measurements, all other nine eye-related measurements were found to be asymmetric, with their frequency distributions not deviating significantly from normal in the Kolmogorov-Smirnov tests ($p > 0.2$ in all cases). To graphically view this, we plotted the asymmetry of eye to pectoral fin against TL (Fig. 8). Although pronounced, the fluctuating asymmetry is not correlated with size, sex, or environment (e.g., being from black vs. white waters). The eye of *O. tamandua* is reduced in its overall size and anatomy (e.g., absence of extrinsic eye musculature; Albert, 2001), and this reduction may be correlated with the observed fluctuating asymmetry.

SKELETAL ANATOMY

General comments.— All of the bones comprising the skeleton of *O. tamandua* are markedly cancellous or trabeculated. According to Albert (2001), this is a character of the family Apteronotidae (with a reversal to having a flat laminar bone surface in his *Apteronotus* sensu stricto). However, the degree of

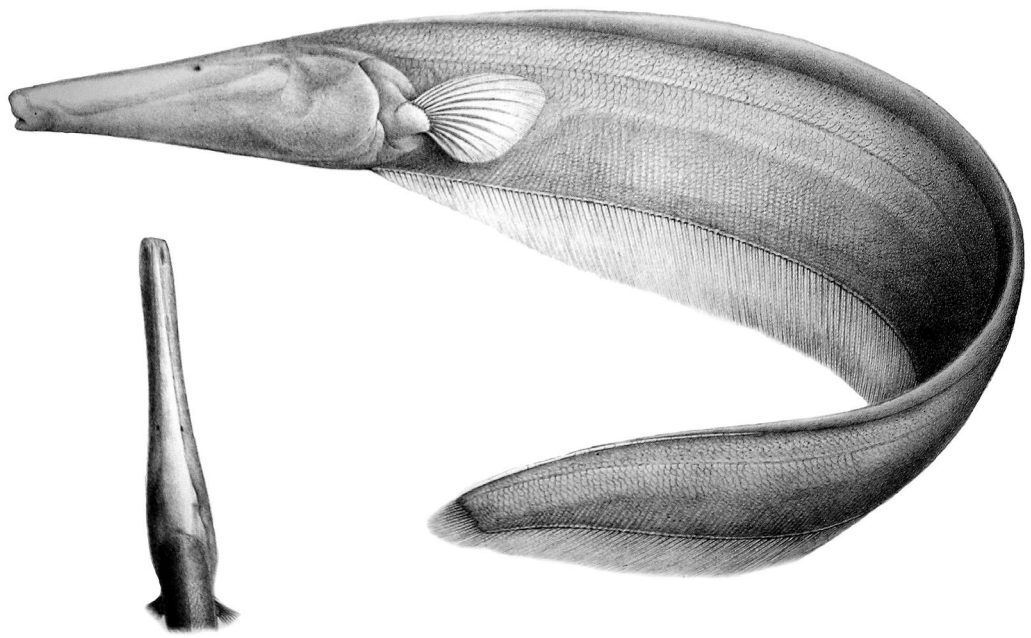

Fig. 2. *Orthosternarchus tamandua*. Figure reproduced from Boulenger (1898: plate 42).

bone trabeculation is extreme in *Orthosternarchus* (Fig. 9), including not only the bones of the skull but those of the post-cranial skeleton (e.g., centra and ribs) as well.

Skull roof and neurocranium.— The skull roof and neurocranium of *O. tamandua* are illustrated in Figure 10. The extremely elongate skull roof is dominated by the paired frontals, which are about 75% of the length of the entire skull. These bones completely surround the anterior fontanelle and form the anterior margins of the posterior fontanelle. The two fontanelles are similar in length, although the anterior one continues posteriorly as a depression formed by the left and right frontals. The parietals form the lateral margins of the posterior fontanelle and contact the frontals anteriorly, the supraoccipital posteriorly, and the pterotics laterally. There is a small ridge of bone that transverses the parietal at the point of contact (or fusion) with the extrascapulars, which also demarcates the anterior insertion of the body musculature. This point is also marked by the thin inermuscular bones of the epaxial musculature that insert into the latice-like surface of the parietals.

The occipital region of the braincase consists of the median supraoccipital and basioccipital and the paired exoccipitals and epioccipitals. The supraoccipital contacts the parietals anteriorly (although this suture is not clear on most specimens due to the complex trabeculation) and the epioccipitals posterolaterally, and completes the posterior margin of the posterior fontanelle. The supraoccipital is a relatively flat, broad element that has a rounded ridge that marks the insertion point of the epaxial body musculature. The epioccipitals form the posterodorsal corners of the braincase, and contact the supraoccipital medially, the exoccipitals ventrally, and the pterotics anteriorly. The foramen for the vagal nerve opens ventrally near the posterior margin of the exoccipital, dorsal to the cartilage filled portion of the exoccipital-basioccipital suture. The exoccipital contacts the basioccipital ventrally, the pterotic anterodorsally, and the epioccipital posterodorsally. The foramen magnum is bounded laterally by the exoccipitals, dorsally by the supraoccipital and the cartilage pad positioned between the skull and supraneural 3, and ventrally by the basioccipital. The flat lateral margin of the basioccipital contacts the exoccipital (the posterior half of this contact is cartilage filled). Internally, the basioccipital and exoccipitals form a pair of chambers for the lagenar otoliths. On the ventral surface of the neurocranium near the posterior midline of the basioccipital is a small patch of cartilage of unknown homology.

The anterior portion of the braincase, comprising the otic and sphenoid regions of the neurocranium, consists of a median orbitosphenoid and four paired bones (pterotics, pterosphenoids, autosphenotics, and prootics). The pterotics support the horizontal semicircular canals of the inner ear, and form the lateral portions of the skull roof. The *m. levator operculi* attaches to the pterotic ventral to a prominent crest on its lateral surface. The pterotics contact the prootics and exoccipitals ventrally, the epioccipitals posteriorly, the parietals dorsally, and the frontals and autosphenotics anteriorly. The orbitosphenoid is the anteriormost bone of this region, and tapers anteriorly where it meets the posterior cartilage of the ethmoid region. Dorsally, the orbitosphenoid contacts a broad cartilage of the neurocranium and posteriorly it is separated from the pterosphenoid by a segment

Fig. 3. Holotype of *Orthosternarchus tamandua* (Boulenger, 1898); BMNH 1897.12.1.208; 425 mm TL. (A) Whole body and (B) head; both in lateral view with anterior facing left.

of cartilage. The pterosphenoid contacts the orbitosphenoid anteriorly, the parasphenoid ventrally, and is very tightly associated with the frontal dorsally. It forms the medial wall of a foramen that is probably for the superficial ophthalmic ramus of the anterodorsal lateral line nerve (Northcutt, 1989); the sphenotic forms the lateral wall of this foramen, which is hidden in Figure 10 (our identification of this foramen follows from the observation on our cleared and stained specimens of a large nerve that exits the foramen and follows the supraorbital sensory canal for its entire length, but this should be confirmed on additional material). The autosphenotic is a rectangular bone with an anterior projection at its contact point with the pterosphenoid. This projection also forms the attachment site for the *m. dilatator operculi*. The prootics are the largest elements of the braincase, and together with the autosphenotics, form the articulatory facet for the hyomandibular. The prootics support numerous foramina (not all are shown in Fig. 10), and together with the exoccipitals form deep subtemporal fossae on the lateral surfaces of the braincase. The prootics contact the basioccipital, exoccipitals, pterotics, sphenotics, and pterosphenoids through cartilage filled sutures, and directly contact the parasphenoid.

The ethmoid region of *O. tamandua* is very elongate and supports the paired lateral ethmoids and the median mesethmoid and ventral ethmoid. The lateral ethmoids are very small elements that are positioned far posteriorly from the other ethmoid bones, about half the distance between the ventral ethmoid and the orbitosphenoid. The mesethmoid and the ventral ethmoid are positioned near the tip of the snout. The mesethmoid has an elongate membrane bone component (about half the length of the snout) and a small endochondral component near the tip of the snout that forms the articulation surface for the premaxilla. The ventral ethmoid, which is fused to the vomer, is large and supports the anterior articulation between the suspensorium and the neurocranium.

Two dermal bones sheath the ventral surface of the neurocranium: the parasphenoid and vomer. The parasphenoid is very elongate, anteriorly nearly reaching the point of fusion between the vomer and ventral ethmoid and posteriorly contacting the ventral surface of the basioccipital. Dorsally, the parasphenoid contacts the orbitosphenoid, and, through very weakly developed ascending rami, the pterosphenoid and the prootic. The vomer, which is fused anteriorly to the ventral ethmoid (the ontogeny of

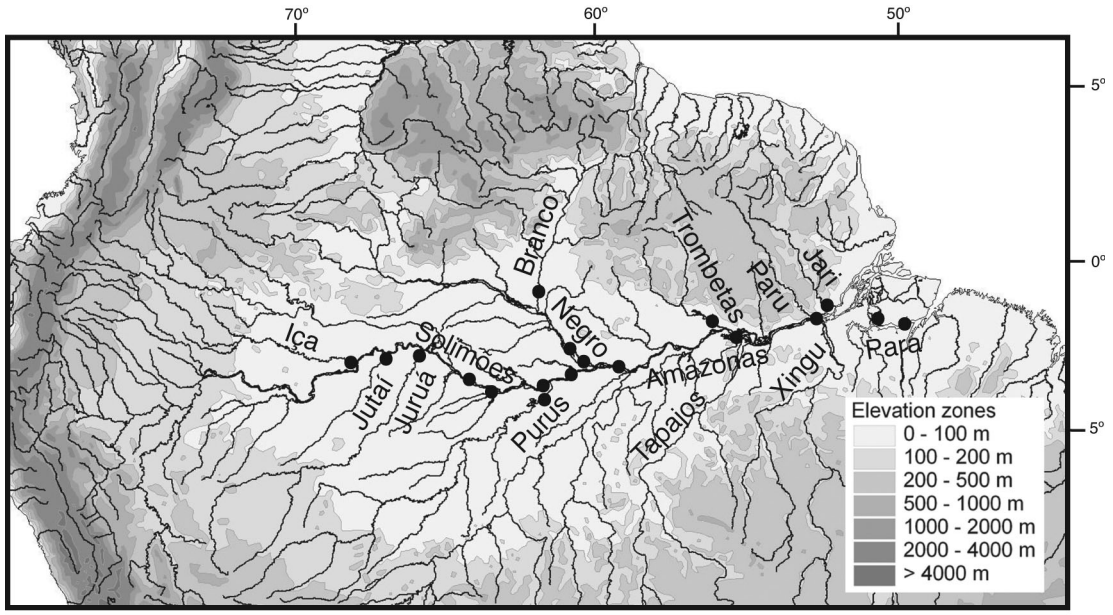

Fig. 4. Map showing the distribution of collection locations of *Orthosternarchus tamandua*. Base map of drainages and elevations provided by Conservation Science Program, World Wildlife Fund US.

this compound element is unknown in *O. tamandua*), is about 1/3 the length of the snout, and posteriorly overlaps ventrally the parasphenoid. The posterior portion of the vomer tapers to a point and sets in a groove in the parasphenoid.

Cephalic sensory canals and their ossifications.— The cephalic lateral line system of *O. tamandua* was diagramatically illustrated by Albert (2001: fig. 19). The bones of the cephalic sensory canal system comprise small, tubular ossifications that surround the sensory canal itself. There are between six and nine ossifications of the supraorbital sensory canal, which are lateral to and remain separate from the frontal (Fig. 10). These are shorter further anterior on the snout, and none is recognizable as a nasal. Even when the numbers of ossifications are equal between the left and the right sides, they are asymmetrical in size and position. There are three to five ossifications of the supratemporal sensory canal (e.g., the extrascapular ossifications). These bones are variable and asymmetrical in number and are mostly free, but may also be fused to the underlying parietals. The bones of the infraorbital sensory canals number between 14 and 16 and become shorter further anterior on the head where the canal turns dorsally at the tip of the snout to curve around the maxillary articulation (Fig. 11). The dorsalmost of the series is consistently curved ventrally. As with those of other sensory canals, the infraorbital ossicles are bilaterally asymmetrical in size, position, and sometimes number. The bones of the mandibular and preopercular sensory canal remain autogenous from their underlying bones (i.e., the preopercle, angular, and dentary) and number between 10 and 14 individual elements; three to five of these are associated with the preopercle. As in the supraorbital and infraorbital canals, the ossicles become smaller anteriorly (Fig. 11).

Suspensorium and oral jaws.— The suspensorium of *O. tamandua* consists of the ossifications of the hyosymplectic (hyomandibular, symplectic) and the palatoquadrate (quadrate, metapterygoid, endopterygoid) cartilages (Fig. 11). The long axis of the hyomandibular is strongly oblique (i.e., nearly horizontal), and laterally overlaps the preopercle. The neurocranial articulatory head of the hyomandibular is rounded. The opercular articulatory head is nearly indistinct from the main body of the hyomandibular and is directed posteroventrally. The foramen for the hyomandibular trunk of the facial nerve is positioned near the base of the neurocranial articulatory head. A second foramen for a branch of this nerve is also prominent, and entirely within the body of the hyomandibular. The elongate symplectic is anteroventral to the hyomandibular and a small area of cartilage separates the two bones. The symplectic sits in a pocket formed by the quadrate and the preopercle, and is visible in lateral view.

The ossifications of the palatoquadrate curve dorsally to form the roof of the mouth. The quadrate is the largest bone of the palatoquadrate, and its anterior and posterior margins of the quadrate are straight, whereas the cartilage-filled dorsal margin is smoothly arched. The posteroventral process of the quadrate is distinct, although in lateral view it is covered by the preopercle. The metapterygoid is positioned posterodorsal to the quadrate and also contacts the anterior edge of the hyomandibular. The endopterygoid overlaps both the quadrate and metapterygoid medially. The anterior portion of the palatoquadrate cartilage (the

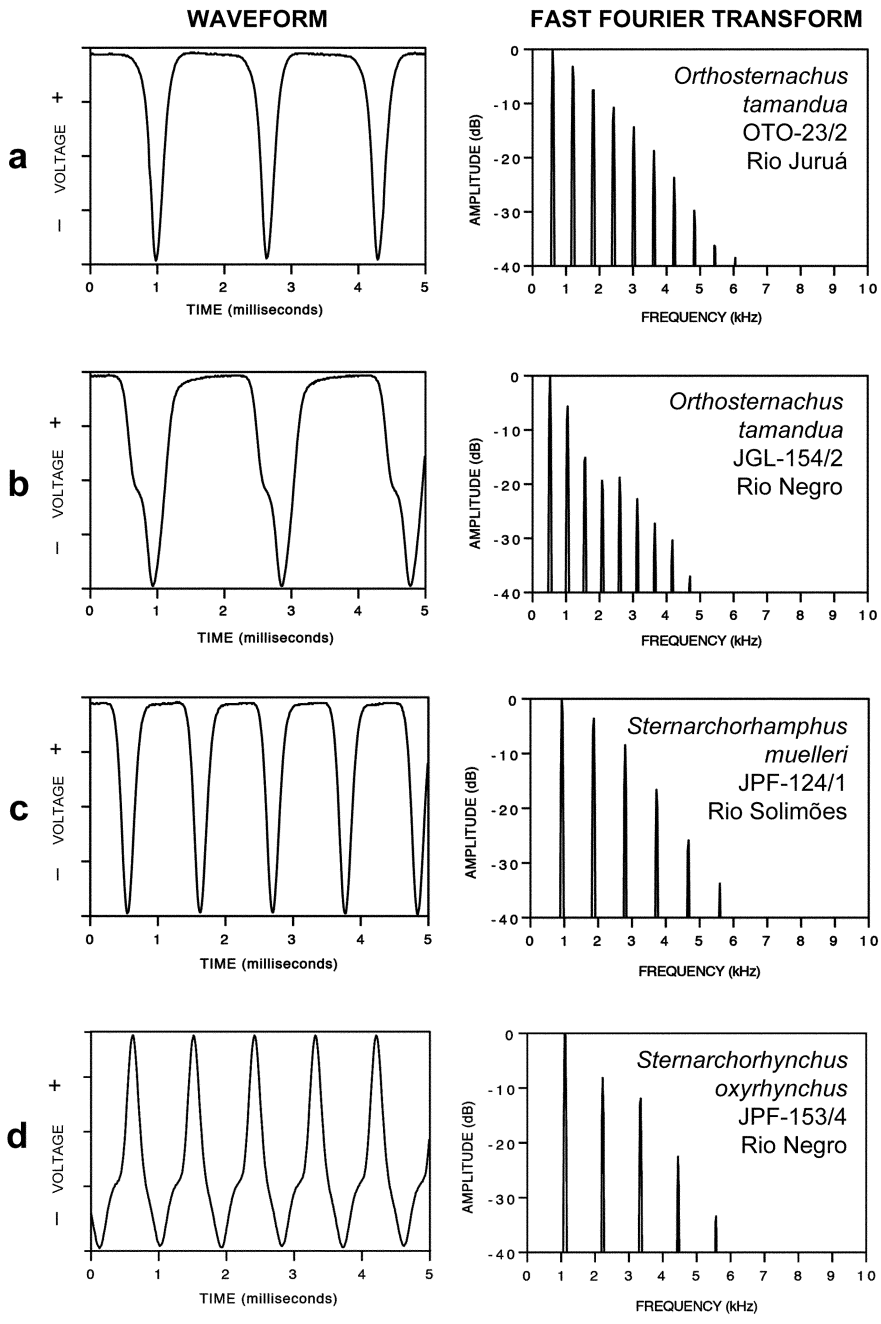

Fig. 5. Electric organ discharge waveforms and their frequency content shown by fast Fourier transforms from (A, B) *Orthosternarchus tamandua*, (C) *Sternarchorhamphus muelleri*, and (D) *Sternarchorhynchus oxyrhynchus* recorded during the 1993 Calhamazon Expedition on the Amazon River and its tributaries. Head positivity shown upwards. Recordings were AC-coupled, so point of zero-crossing on voltage axis is unknown. Specimen ID and collection locality are indicated. The EODs of both *O. tamandua* and *S. muelleri* consist of head-negative spikes superimposed over a head-positive baseline unlike the biphasic EODs of other apteronotid gymnotiforms, such as *S. oxyrhynchus*. However, the repetition rate of the EOD is much slower in *O. tamandua* than for *S. muelleri*.

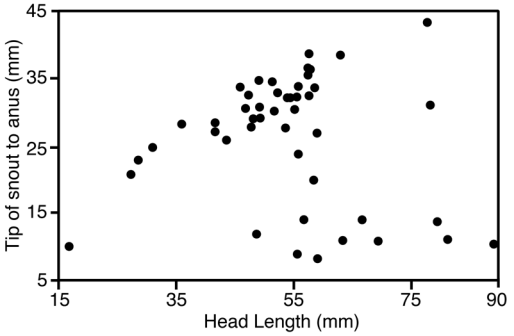

Fig. 6. Relationship between position of anus and head length for a sample of 47 specimens of *Orthosternarchus tamandua*.

pars autopalatina) curves laterally to contact the cartilaginous articular head of the maxilla.

The *m. levator operculi*, *m. dilatator operculi*, and *m. adductor mandibulae* all have intermuscular ossifications, which appear to become denser in number and more heavily ossified during ontogeny (although they are always filamentous; Fig. 11). In the smallest cleared and stained specimen examined (FMNH 117281, 155 mm TL), these bones are well developed and numerous in the *m. adductor mandibulae* and *m. levator operculi*, but there are only a few isolated bones in the *m. dilatator operculi*. In the larger cleared and stained individuals examined, they were more numerous in the *m. dilatator operculi* than in the *m. levator operculi*. Similar intermuscular bones are also present in the *m. adductor mandibulae* of *Rhamphichthys* (J. S. Albert, pers. comm. 2005), and may be correlated with an elongated snout (although this does not explain their presence in the opercular muscles of *O. tamandua*).

The edentulous maxillae of *O. tamandua* are elongated, with a long, tapering posterior tip (Fig. 12). The anterior (ventral) margins of the maxillae are smoothly curved and there is a cartilaginous articular surface on its dorsal margin. Albert (2001) described the maxillae of *O. tamandua* as possessing an anterior shelf of the descending blade and noted that its ventral margin was not ossified (both of these characters were considered autapomorphic for the genus). The premaxillae are flattened, and are relatively featureless except for a distinct concavity on their dorsal surfaces near the medial edge that serve as the articulation site for the ethmoid region of the neurocranium.

The bones of the lower jaws (Fig. 12) consist of the dentary, anguloarticular, retroarticular, coronomeckelian, mentomeckelian, and a series of six to nine tubular ossifications of the mandibular sensory canal that remain separate from their underlying bones (i.e., the anguloarticular and dentary). The anterodorsal margin of the dentary is slightly curved and its posterior margin its distinctly forked. There are four or five rows of teeth on the dentary that are restricted to the anterior portion of the bone. Meckel's cartilage is very robust posteriorly where it contacts the articular. Near the anterior tip of Meckel's cartilage is a distinct mentomeckelian, which appears to be a collar of perichondral bone. The coronomeckelian is a sliver of bone that forms at the apex of Meckel's cartilage just anterior to its contact with the articular. The articular and retroarticular contribute equally to the articulatory facet, and the retroarticular tapers to a point posteriorly.

Opercular series.— The opercular series of each side consists of a preopercle, opercle, subopercle, interopercle, and two branchiostegals (Fig. 11). The preopercle is closely associated with the posteroventral margin of the hyomandibular. There are between three and five tubular ossifications of the preopercular sensory canal that are aligned with the ventral margin of the preopercle, but which remain autogenous from the preopercle (i.e., the preopercle itself does not support the sensory canal). The opercle is shield-shaped, with a concave dorsal margin that is somewhat flattened for the insertion of the *m. levator operculi*. There is a lateral flange originating from the point of the facet for the hyomandibular that separates the insertion sites of the *m. dilatator operculi* and *m. levator operculi* (i.e., demarcates the anterior extent of the attachment of the *m. levator operculi* to the opercle). The interopercle is long, extending from the anterior margin of the opercle to the anterior point of the preopercle and almost reaching to lower jaw. It is relatively broad, but tapers slightly anteriorly, and is rounded at both ends. The subopercle is also long and broad, and is very similar in form to the posteriormost branchiostegal. Its anterior end is loosely associated with the posterior ceratohyal, and it is positioned medial to the opercle and interopercle, although its ventral margin is visible in lateral view (Fig. 11A). There are only two branchiostegals in *O. tamandua* (Fig. 13). The anterior branchiostegal is extremely slender and thread-like and articulates with the ventral margin of the anterior ceratohyal. In contrast, the posterior branchiostegal is much broader and closely resembles the shape of the subopercle and only loose contacts the lateral surface of the anterior and posterior ceratohyals.

Gill arches and ventral portions of the hyoid arch.— The gill arches of *O. tamandua* are illustrated in Figure 14. Each side of the dorsal branchial skeleton consists of five epibranchials (eb1-5), three infrapharyngobranchials (ipb 2-4), and a pharyngobranchial toothplate (uptp). [For comparisons to recent gymnotiform literature, e.g., Albert, 2001, note that we use the numbering system of the branchial arches typically used in anatomical studies of actinopterygian fishes (e.g., beginning with the first branchial arch)]. All elements of the dorsal branchial skeleton are ossified, except for eb5 and iph4. Epibranchial 3 bears a thin but prominent uncinate process, and eb4 is forked posteriorly with each prong contacting eb5. Together eb4 and eb5 form a wide foramen. The small, circular uptp, which is supported by iph4 and eb4 and bears about three rows of teeth with two to four teeth per row.

The ventral branchial skeleton consists of three hypobranchials (hb1-3), five ceratobranchials (cb1-5), and the basibranchial skeleton, which has two ossified basibranchials (bb2, 3) and an anterior element that positionally, at least, may be identified as a fused basihyal and first basibranchial (bh+bb1), although the ontogeny of this element is unknown. The anterior tips of the left and right hb1 are positioned ventral to bh+bb1, but do not contact each other. The ceratobranchials are the longest elements of the branchial arches, and are simple bars of bone,

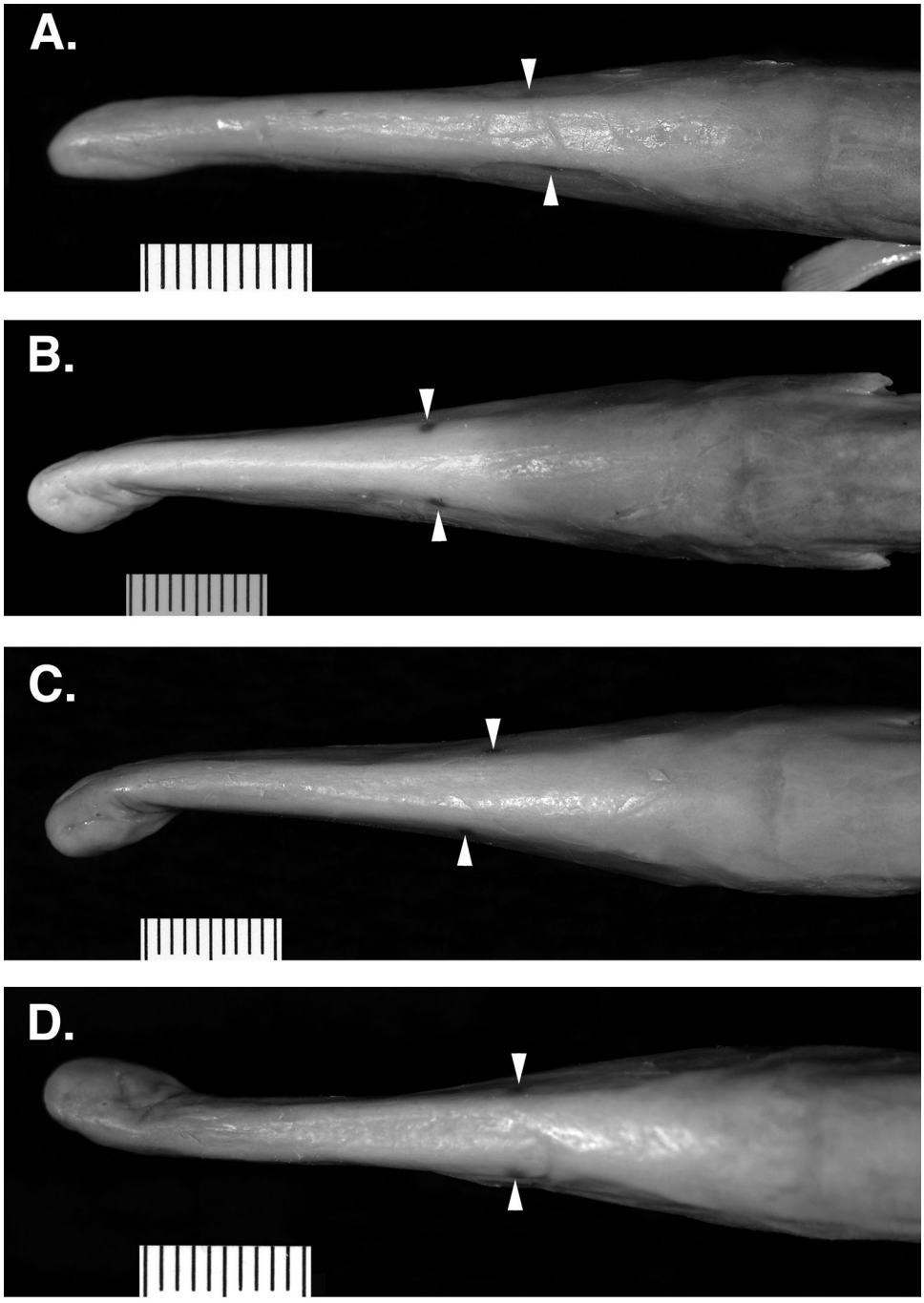

Fig. 7. Heads of four specimens of *Orthosternarchus tamandua* in dorsal view showing asymmetry in the position of the eyes (indicated by white arrow heads). (A) FMNH 114913, 316 mm TL). (B) FMNH 114912, 354 mm TL). (C) FMNH 114912, 377 mm TL). (D) FMNH 114910, 331 mm TL). Scale bars in millimeters. Anterior facing left.

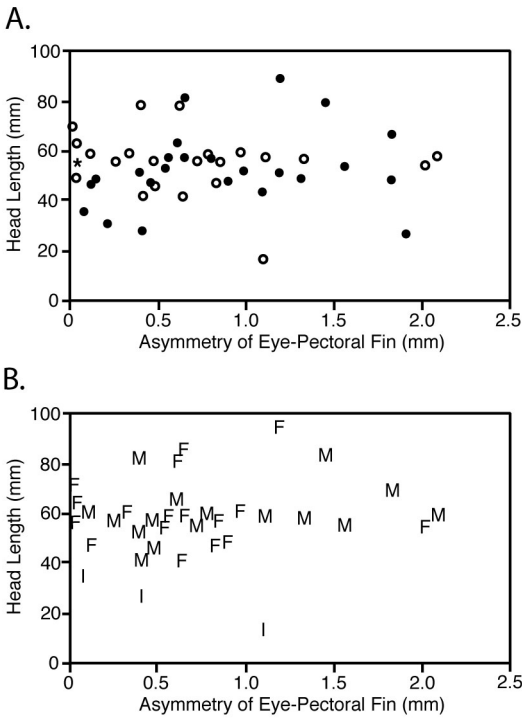

Fig. 8. Bilateral asymmetry of the position of the eyes plotted against head length for a sample of 47 specimens of *Orthosternarchus tamandua*. (A) values plotted according to type of water in water in which specimens were taken: solid circles indicate specimens from black water environments, open circles from white water environments, and asterisk from clear water environments. (B) values plotted according to sex of individual: M, male; F, female; I, immature.

with the exception of cb4, which is relatively broad posteriorly, and cb5, which bears a medial patch of teeth. Ceratobranchial 5 is also out of plane from the other elements of the series, and is oriented obliquely with the posterior tip displaced dorsally. The anterior tip of cb5 consequently is ventral, and contacts the cartilaginous posterior basibranchial (bb4), which is curved ventrally. In all the cleared and stained specimens available, there was found to be a small cartilaginous nodule dorsal to the contact between bb4 and cb5 (Fig. 14). The gill rakers are very simple in form, being mere flecks of bone in the cleared and stained specimens, and are almost entirely restricted to the ventral portions of the branchial arches (there may be only one or two gill rakers, if any, associated with the dorsal elements).

Closely associated with the gill arches are the ventral portions of the hyoid arch (i.e., interyhyals, hypohyals, and the anterior and posterior ceratohyals). The interhyal is an extremely small ossification and there is no trace of a cartilaginous component of this element at the stages we studied. The posterior ceratohyal has a rounded posterior margin and a distinct notch ventrally. This notch is filled by a cartilage that forms a portion of the ventral margin of the hyoid arch and the junction between the anterior and posterior ceratohyals. The anterior ceratohyal is hatchet shaped and anteriorly contacts both the dorsal and ventral hypohyals (separated by a small area of cartilage). The hypohyals contact the bh+bb1 at about the midpoint of the element (indicated by an arrow in Fig. 14). The urohyal is extremely elongate and is roughly shaped like an inverted T in cross section. Posteriorly, it becomes filamentous, and there are several slivers of bone associated with the urohyal that are loose in the *m. sternohyoideus*.

Weberian apparatus.—The skeletal portions of the Weberian apparatus of *O. tamandua* are illustrated in Figure 15. As in other Gymnotiformes, the Weberian apparatus in *O. tamandua* is relatively simple compared to other ostariophysan fishes (e.g., the absence of a claustrum, Britz and Hoffmann, 2006). This region of the skeleton was not very clear on the cleared and stained specimens (e.g., details were obscured by numerous filamentous intermuscular bones and, upon dissection this region became polluted with perilymph and small fragments of the intermusculars). Further study must be made of the Weberian apparatus of *O. tamandua* and other taxa for comparisons among apteronotid fishes. Such a study should prove interesting given the phylogenetically informative nature of this region in ostariophysan fishes generally (e.g., Fink and Fink, 1981; Britz and Hoffman, 2006; Hoffmann and Britz, 2006).

The neural arches of the third and fourth vertebrae and the median supraneural 3 are the largest autogenous bony elements of the Weberian apparatus, and all meet one another through cartilage-filled sutures to form a roof to the anterior neural canal, similar to the arrangement illustrated for *Sternopygus* by Fink and Fink (1981). The supraneural 3 of *O. tamandua* is adjacent to the supraoccipital and the exoccipitals, from which it is separated by a pad of cartilage; neural arch 3 is adjacent to the exoccipitals.

The exact shape and size of the scaphium is not entirely clear on our cleared and stained specimens, but it appears to be a small ossification positioned anterior to, and slightly lateral to the ventral portion of neural arch 3. The intercalarium is a tiny intraligamentous nodule of bone, similar to that of other gymnotiforms (e.g., *Sternopygus*, Fink and Fink, 1981: fig. 18), and is positioned medial to the anterior tip of the tripus. The tripus is narrow anteriorly, but is wide in its midsection where it supports a median cartilaginous region (not shown in Fig 15) and tapers again posteriorly at the point where it passes through an opening delimited by a bridge between the dorsal wing-like expansion and expanded parapophysis of the fourth vertebra (see below).

The first centrum is extremely compressed and is very much disk-like. The second centrum is slightly larger, and bears a prominent pair of expanded parapophyses that extend laterally from the centrum but are then bent posteriorly. The third centrum is largely obscured from view by the other components of the Weberian apparatus, but it can be seen to broadly and closely contact its neural arch along its anterodorsal margin, and approaches the neural arch of the fourth centrum along its posterodorsal margin. The fourth vertebra is the most elaborate of the Weberian apparatus. Its autogenous neural arch sutures through cartilage anteriorly to supraneural 3 and the third neural arch, and ventrally to the fourth centrum. Laterally the fourth

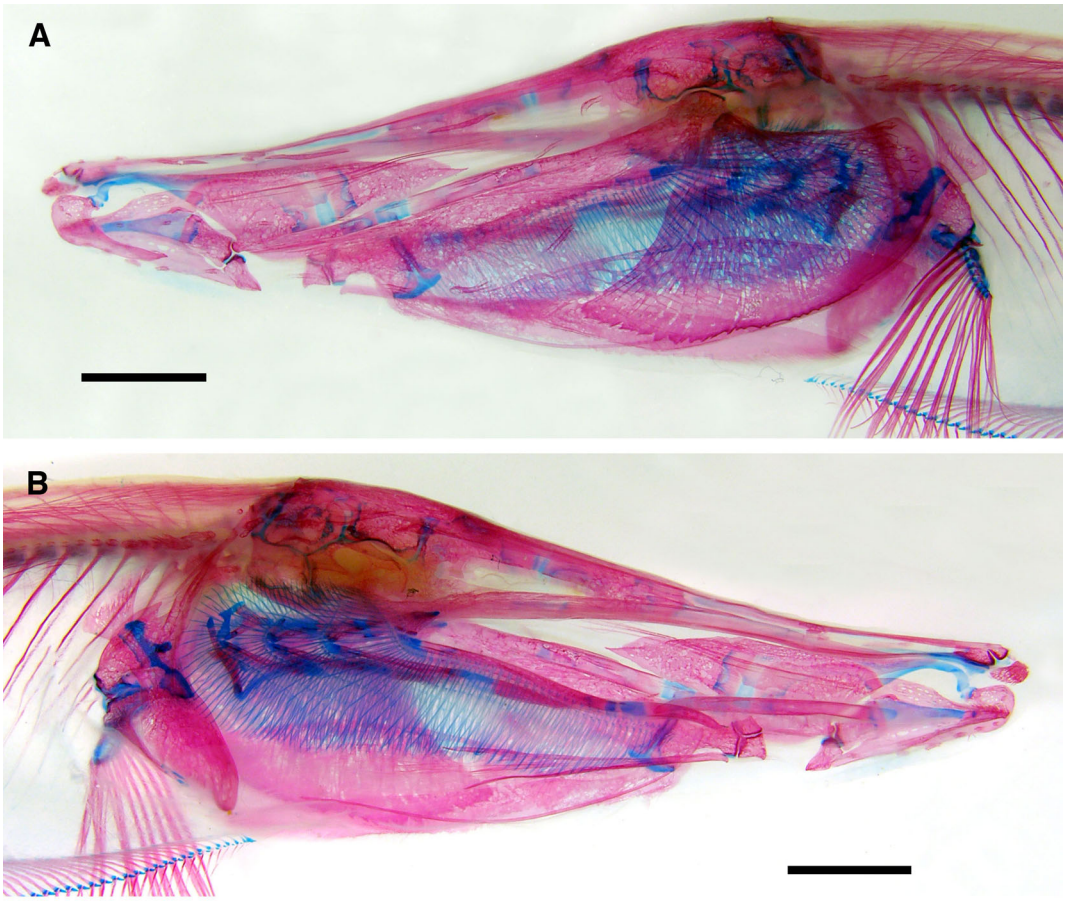

Fig. 9. Skull of cleared and stained specimen (FMNH 117281, 155 mm TL) in (A) lateral and (B) medial views. The right oral jaws, suspensorium, opercular bones, and pectoral girdle have been dissected away from this specimen to show the branchial arches in situ in B. Scale bars = 5 mm. Anterior facing left in A; anterior facing right in B.

centrum supports a dorsal, posteriorly directed wing-like projection, which, with a similar projection from the fifth vertebra, forms the dorsal limitation of a trough-like space. The ventral limitation of this space is defined by the dorsal surface of the greatly expanded fourth parapophysis (= pp4 + rib of Fink and Fink, 1981) and the expansion of the fused rib and parapophysis of the fifth vertebra (see below). The expanded fourth paraphophysis appears to act as a brace for the pectoral girdle (at the point where the supracleithrum and cleithrum overlap) and, in ventral view, is roughly triangular in shape and slightly concave.

Although not technically part of the Weberian apparatus (i.e., the complex modification and connections of the first four vertebrae in otophysan fishes, along with the perilymphatic system and swimbladder of this region), the fifth vertebra of *O. tamandua* is also greatly modified (compared to more posterior abdominal vertebrae), and is described here, as this modification is likely associated with the Weberian apparatus. There is a distinct posteriorly directed dorsal expansion from the lateral surface of the centrum, similar to that found on the fourth vertebra. The rib of the fifth vertebra, which is only slightly shorter than the more posterior ribs, is fused to the parapophysis and contributes to a broad, wing-like expansion that is smoothly curved and strongly concave ventrally. The next posterior vertebra lacks any expansion of either the parapophyses or ribs, and the constituent elements (i.e., rib, paraphophyses, and centrum) are autogenous.

Vertebral column.— There are 16-17 abdominal vertebrae (20-21 including the Weberian vertebrae) and 67-89 caudal vertebrae (n=21). Most of the observed variation in the number of caudal vertebrae is reflective of the regeneration that is common in apteronotid fishes generally and our counts are likely low. For instance, in an apparently complete (i.e., unregenerated) cleared and stained specimen (FMNH 117281), we counted 94 caudal vertebrae. There is substantial variation in the anatomy of the vertebrae between the abdominal and caudal regions (Fig. 16).

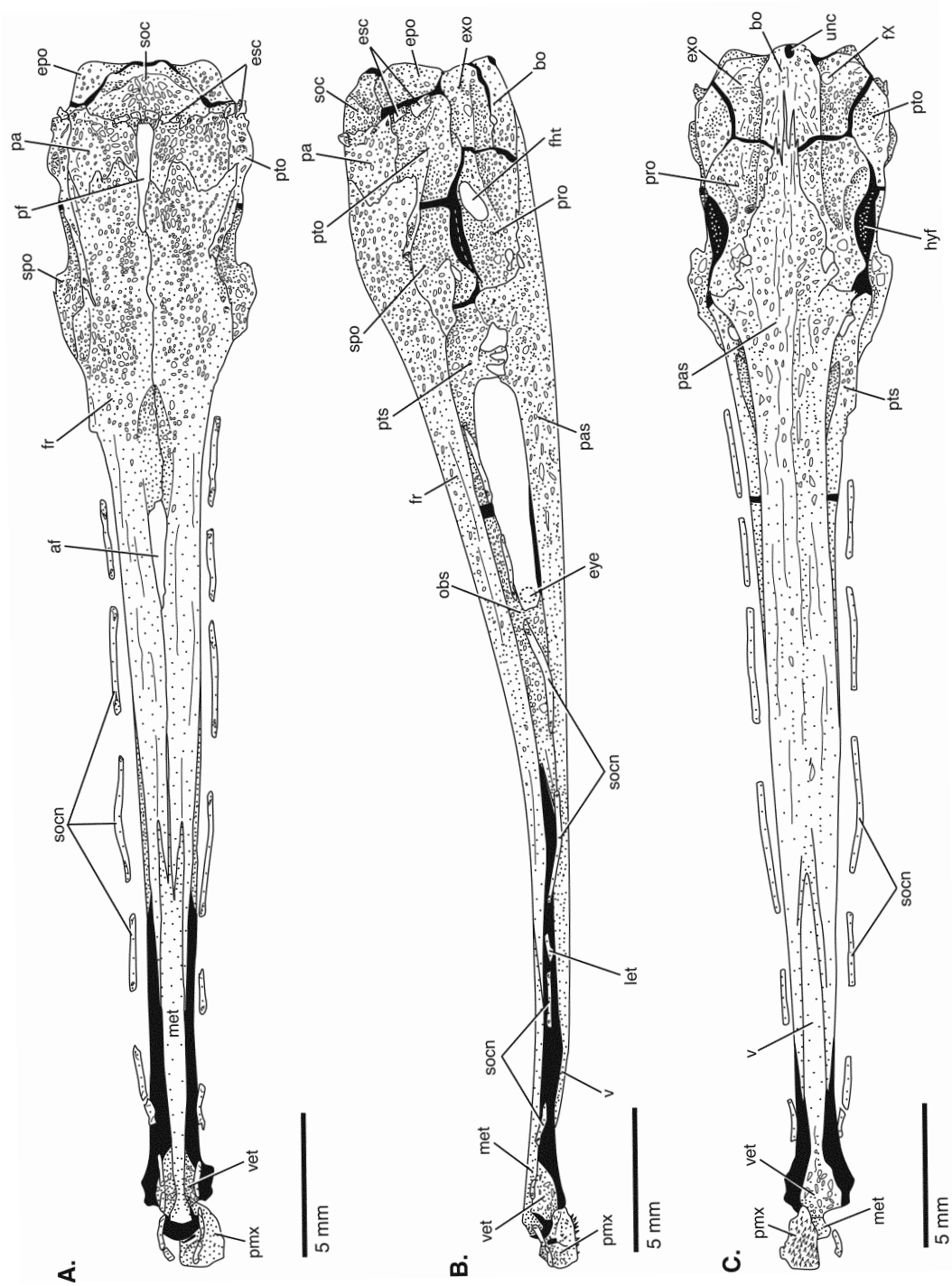

Fig. 10. Skull roof and braincase in (A) dorsal, (B) lateral, and (C) ventral views; ANSP 187028, 205 mm TL. Anterior facing bottom of the page. Abbreviations: af, anterior fontanelle; bo, basioccipital; epo, epioccipital; esc, extrascapular (ossification of the occipital sensory canal); fr, frontal; hyf, articular surface for neurocranial head of hyomandibular; let, lateral ethmoid; met, mesethmoid; obs, orbitosphenoid; pa, parietal; pas, parasphenoid; pf, posterior fontanelle; pmx, premaxilla; pro, prootic; pto, pterotic; pts, pterosphenoid; soc, supraoccipital; socn, ossifications of the supraorbital sensory canal; spo, sphenotic; unc, unidentified cartilage; v, vomer; vet, ventral ethmoid.

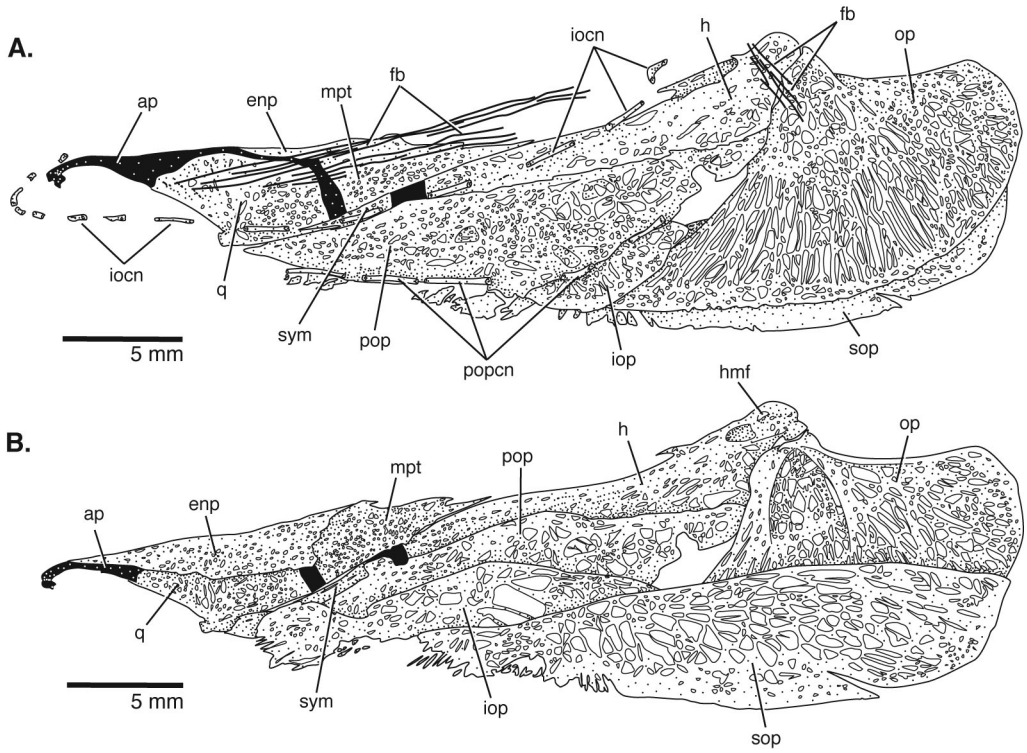

Fig. 11. Suspensorium and opercular bones from the right side in (A) lateral and (B) medial views; ANSP 187028, 205 mm TL. Anterior facing left (images in A reversed). Abbreviations: ap, *pars autopalatina* of palatoquadrate cartilage; enp, endopterygoid; fb, filamentous bone; h, hyomandibular; hmf, foramen for hyomandibular trunk of facial nerve; iocn, ossifications of the infraorbital sensory canal; iop, interopercle; mpt, metapterygoid; op, opercle; pop, preopercle; popcn, ossifications of the preopercular sensory canal; q, quadrate; sop, subopercle; sym, symplectic.

However, there are also some noteworthy features common to vertebrae no matter the region. For instance, the neural arches are positioned anteriorly on the centrum, to which they are fused. Posterior to the neural arches, there is a second, much lower process that may contact the neural arch of the next posterior vertebra, effectively forming a zygopophysis. The neural spines are oblique to the body axis and span about three vertebrae. This orientation stands in contrast to the hemal spines, which are nearly vertical. The hemal arches and spines are, as with the neural arches, positioned on the anterior portion of their respective centrum. In the abdominal region, there is a remnant cartilage of the basiventrals associated with all post-Weberian parapophyses except the posteriormost (cartilages not shown in Fig. 16). Most of the parapophyses (i.e., the ossifications of the basiventrals) are relatively short, although the posteriormost two are somewhat elongate. The parapophyses are autogenous and separate from the centra relatively easily, although there may be thin dermal bone trabeculations that join the parapophyses to the centra, particularly anterodorsally. The ribs are all (posterior to the Weberian apparatus) uniform in size except for the posteriormost two, which are slender and much smaller. All ribs have cartilaginous distal tips, and articulate with the parapophyses.

The intermuscular bones of *O. tamandua*, as in other apteronotids, are extensive and extremely complex, and function to greatly stiffen the laterally compressed body. The most superficial of the primary series of intermuscular bones are the dorsal and ventral series of myorhabdoi (myb(d) and myb(v), respectively; Fig. 16D). These are bony rods with frayed anterior and posterior ends. The solid rod portions of these elements lie immediately beneath the skin, while the frayed ends are deeper in musculature (and are deep to the epicentral bone in the dorsal series). The dorsal series continues as robust elements anteriorly to the back of the skull, whereas the elements of the ventral series become much smaller anteriorly in the abdominal region. Our terminology for these elements (i.e., identification as myorhabdoi) follows from Patterson and Johnson (1995), although it is possible they are modified epineural and epipleural bones (dorsal and ventral series, respectively), although we were unable to trace their relationship to individual myosepta. Throughout the abdominal region, and extending posteriorly about two-thirds

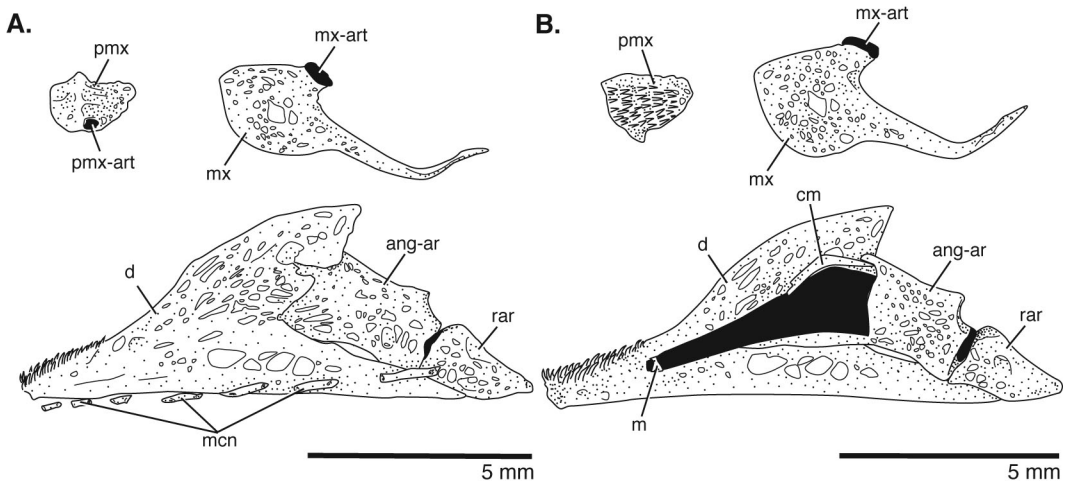

Fig. 12. Oral jaws from the right side in (A) lateral (premaxilla in dorsal) view and (B) medial (premaxilla in ventral) view; ANSP 187028, 205 mm TL. Anterior facing left (images in A reversed). Abbreviations: ang-ar, anguloarticular; cm, coronomeckelian; d, dentary; m, mentomeckelian; mcn, ossifications of the mandibular sensory canal; mx, maxilla; mx-art, articulatory head of maxilla; pmx, premaxilla; pmx-art, articulatory surface of the premaxilla; rar, retroarticular.

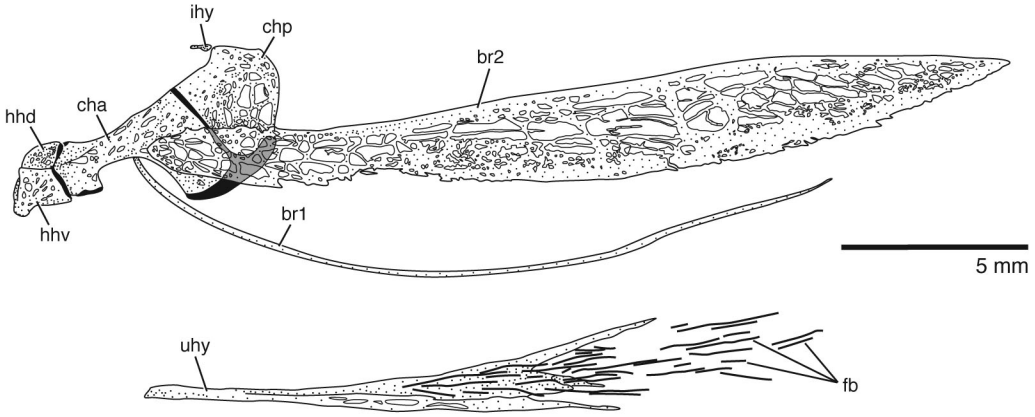

Fig. 13. Elements of the ventral hyoid arch in lateral view; ANSP 187028, 205 mm TL. Bone shown in white, cartilage in black (except where overlain by br2, where it is shown in gray). Branchiostegals are illustrated slightly out of position and spread apart for clarity. Anterior facing left. Abbreviations: br, branchiostegal; cha, anterior ceratohyal; chp, posterior ceratohyal; fb, filaments of intermuscular bone; hhd, dorsal hypohyal; hhv, ventral hypohyal; uhy, urohyal.

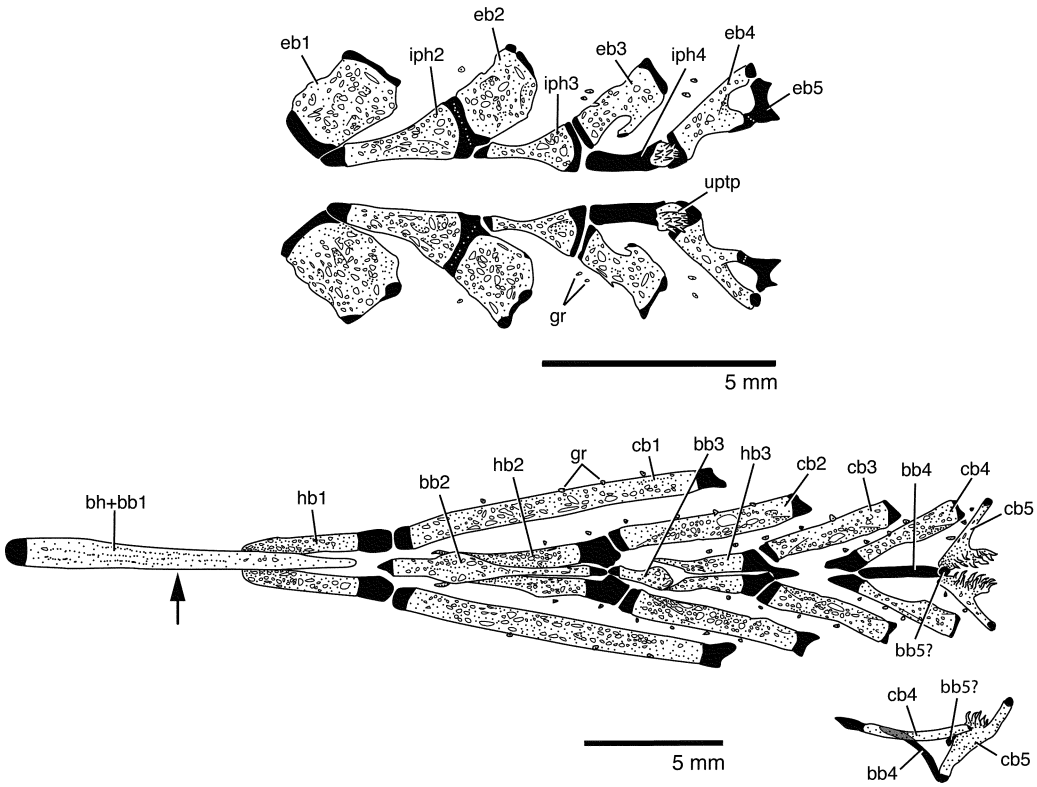

Fig. 14. Dorsal (top) and ventral (bottom) gill arches in oral view (i.e., dorsal gill arches in ventral view and ventral gill arches in dorsal view); ANSP 187028, 205 mm TL. Inset below ventral gill arches shows the posterior portion of ventral gill arches in lateral view. Arrow indicates position at which hypohyals contact basihyal-basibranchial 1. Anterior facing left. Abbreviations: bb, basibranchial; bh, basihyal, cb, ceratobranchial; eb, epibranchial; gr, gill raker; hb, hypobranchial; iph, infrapharyngobranchial; uptp, upper pharyngeal toothplate.

along the length of the caudal region, is a series of epicentral bones. These arise in the horizontal septum (confirmed on cleared and stained specimens placed in 70% ethanol), and in the abdominal region they attach, either directly or through a ligament, to the parapophyses. The horizontal septum splits laterally where it contacts the skin to form a trough housing the large lateral line nerve bundle. The epicentrals bend dorsally, which is particularly evident anteriorly in the series where they are longest. There is a branch of the epicentral in the ventral portion of horizontal septum, so that the epicentrals bracket the lateral line nerve. This ventral branch may or may not fuse to the dorsal epicentral bone (fusions are more typical in the anterior portion of the body; cf. Fig. 15A and Fig. 16D). Small filamentous bones are distributed throughout the body musculature. In small individuals (e.g., FMNH 117286, 155 mm TL) these seem to be arranged more or less in seven series (one median dorsal series and three bilaterally paired series), although in larger individuals (e.g., ANSP 187028, 205 mm TL) they become much denser throughout the body musculature and the boundaries between the series are obscured. The ventralmost series (fb(v)) forms in the ligamentous tissue separating the hypaxial body musculature from the anal fin musculature.

Caudal fin and supports.— The caudal skeleton and fin of most specimens has been regenerated and shows great teratological variation (e.g., Fig. 17B). In the one cleared and stained specimen examined in which the caudal skeleton is complete there is a simple cartilaginous hypural plate that supports nine caudal fin rays (FMNH 117281; Fig. 17A). The hypural plate is separated from the last anal fin pterygiophore by 13 vertebrae. In the regenerated tail (Fig. 17B), the hypural plate is continuous with the terminal vertebral centrum, and a series of regenerated fin rays is intercalated between the anal and caudal fins, forming a continuous anal-caudal fin.

Posteroventral abdominal bone.— The posteroventral abdominal bone (Fig. 16; = rib-like bones of Lundberg and Mago-Leccia, 1986; displaced hemal spine of Albert, 2001) of *O. tamandua* is well-developed and supports the posterior and most of the ventral margins of the abdominal cavity. It is roughly T shaped in cross section, and its proximal end is in contact with

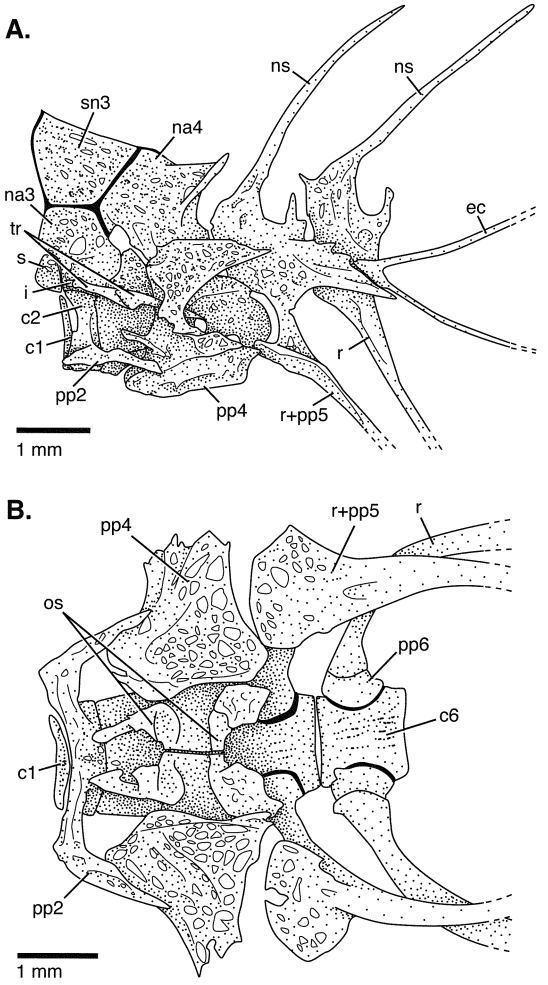

Fig. 15. Weberian apparatus (anterior vertebrae) in (A) lateral and (B) ventral views; ANSP 187028, 205 mm TL. Anterior facing left. Abbreviations: c, centrum; ec, epicentral intermuscular bone; i, intercalarium; na, neural arch; ns, neural spine; os, os suspensorium; pp, parapophysis; r, rib; s, scaphium; sn3, supraneural three; tr, tripus.

the first hemal arch and its associated displaced haemal spine (hs1, Fig. 16B), being positioned between the anterolateral flanges of the hemal arch.

The posteroventral abdominal bone of other apteronotids is similar in shape to that illustrated here for *O. tamandua*, although there is variation in this element within Gymnotiformes (e.g., Albert, 2001: figs. 35, 36). Lundberg and Mago-Leccia (1986) noted that certain developmental aspects of these bones in *Sternopygus* were reminiscent of ribs (e.g., position off the midline, details of chondrification and ossification). In contrast, Albert (2001) concluded that there was little support for the homology of this bone with ribs, in part citing evidence from observations of the development of this bone in *Apteronotus leptorhynchus*. Although these brief mentions of the development of the posteroventral abdominal bone have been made, the ontogeny of these structures needs to be better studied in Gymnotiformes, and such study may be informative for this homology statement.

Dorsal fin and supports.— These elements are completely absent in *O. tamandua*, as in other Gymnotiformes (e.g., Fink and Fink, 1981; Mago-Leccia, 1994).

Anal fin and supports.— In our sample, the anal fin of *O. tamandua* consists of 207-256 fin rays (n=45) although the natural number of supports and fin rays is unknown due to tail loss and regeneration, and, as for the caudal vertebrae, much of the observed meristic variation is due to regeneration. In the one cleared and stained specimen (FMNH 117281) with a complete, unregenerated tail (and for which the small anterior and posterior fin rays could be counted with higher certainty than for alcohol specimens) the anal fin rays numbered 254. All fin rays are segmented and are branched posterior to about fin ray 42; none are branched more than once (towards the posterior end of the fin, some of the fin rays were found to not be branched, but this may be due to regeneration). There are two or three pterygiophores (an individual series of proximal and distal radial elements) between adjacent hemal spines (Fig. 16B, C). The radial supports consist of a series of elongate proximal radials and distal radials. Each fin ray contacts its proximal radial, its distal radial, and the next posterior distal radial. The first proximal radial does not have an associated fin ray or distal radial. Anterior to the tip of the posteroventral abdominal bone there are about 23 proximal radials. These are oriented strongly obliquely (Fig. 16B), but become perpendicular to the body axis by about fin ray 35-37, and towards the posterior end of the body may become obliquely directed in the opposite direction as the very anterior ones. The distal tips of the anteriormost proximal radials are simple rods of bone, whereas from about proximal radial 23 they develop a posterior laminar flange at their distal most tip. Posterior to about proximal radial 34, they bear an anterior and posterior process so that they resemble the hilt of a sword (Fig. 16B, C). These processes become smaller far posterior on the body.

Pectoral fin and girdle.— The pectoral fin comprises 14-15 fin rays (n=40), the first two of which are unbranched. The first fin ray is about one-third of the length of the next fin ray, and is the only one to articulate with the propterygium. The two or three anterodorsalmost branched fin rays are the longest of the pectoral fin. The fin tapers and the posteroventralmost fin rays are shorter and unbranched.

The dermal elements of the pectoral girdle include the posttemporal, supracleithrum, postcleithrum and cleithrum (Fig. 18). The posttemporal is very small and lies flush against the posterolateral surface of the skull at the epioccipital-pterotic suture. Ventrally, the posttemporal contacts the supracleithrum in a flat, overlapping articulation. The elongate supracleithrum also overlaps the posterior margin of the cleithrum and bears a distinct dorsolateral hook. The postcleithrum is a broad, shield-shaped element that is only loosely connected to the rest of the pectoral girdle, floating in tissue covering portions of the first few ribs.

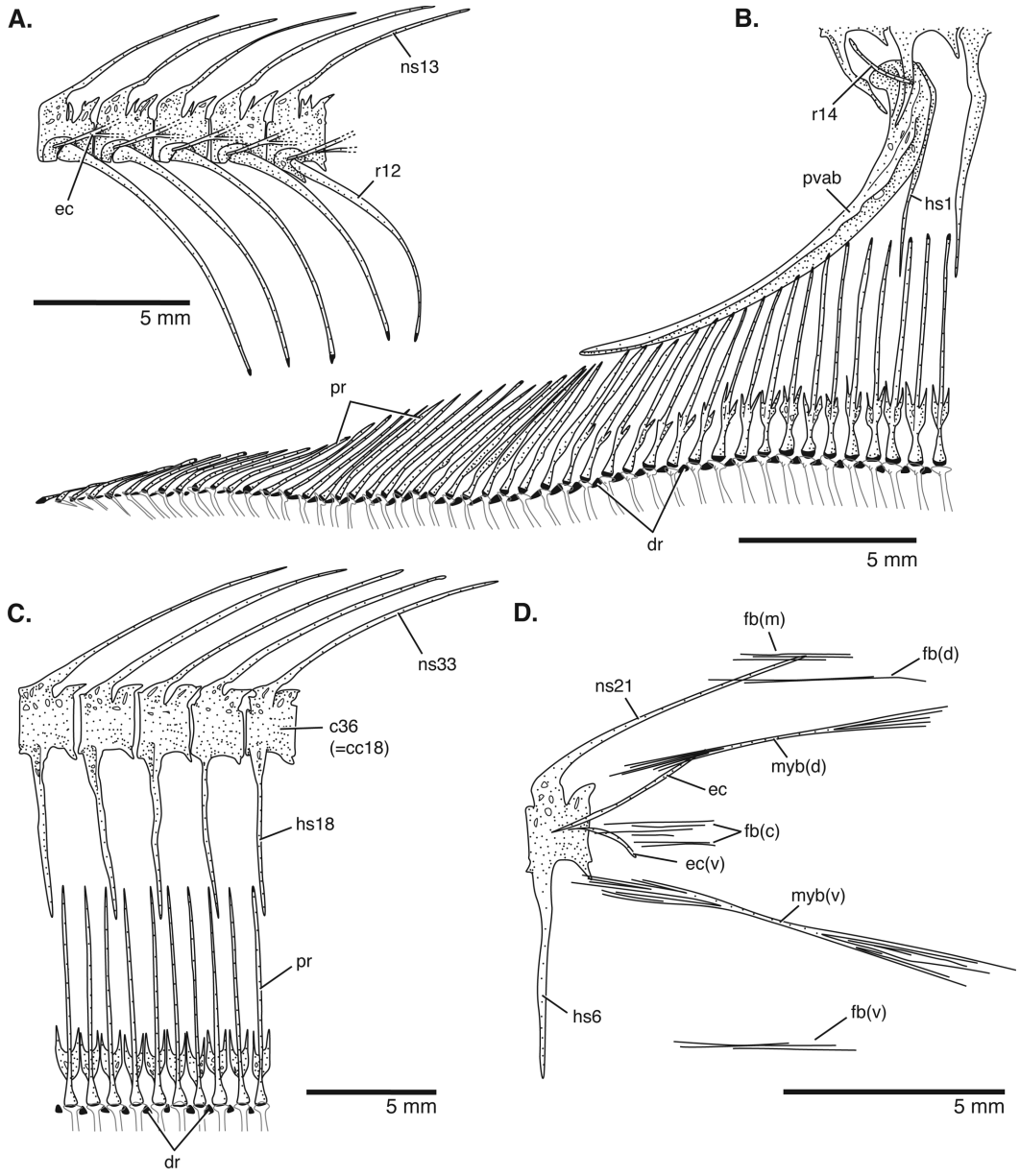

Fig. 16. Elements of the postcranial skeleton illustrated in lateral view; ANSP 187028, 205 mm TL. Anterior facing left. (A) Five abdominal vertebrae. Note that epicentral intermuscular bones have been cut distally. (B) Anterior anal fin supports and the posteroventral abdominal bone. Note that fin rays have been cut distally. (C) Five caudal vertebrae and associated anal fin supports. Note that fin rays have been cut distally and associated intermuscular bones have been omitted. (D) Intermuscular bones associated with each vertebra. Note that the various series of filamentous bones are continuous along the length of the axial skeleton, and it is difficult to determine their relationship to individual myosepta. Abbreviations: c, centrum; cc, caudal centrum; ec, epicentral intermuscular bone; ec(v), ventral branch of epicentral intermuscular bone, which variably are fused to the main epicentral giving this bone a branched appearance; dr, distal radial of anal fin; fb(c), central series of filamentous bones along the flank; fb(d), dorsal series of filamentous bone; fb(m), dorsal median series of filamentous bone; fb(v), ventral series of filamentous bones; hs, hemal spine; myb(d), dorsal myorhabdoi (possibly = epineurals); myb(v), ventral myorhabdoi (possibly = epipleurals); ns, neural spine; pr, proximal radial of anal fin; pvab, posteroventral abdominal bone; r, rib. In this figure, ribs are numbered beginning with the first unmodified rib (i.e., with the rib of vertebrae 5) and neural spines are numbered beginning with the first full neural spine (i.e., in which the left and right neural arches are fused in the midline, which is on vertebra 4).

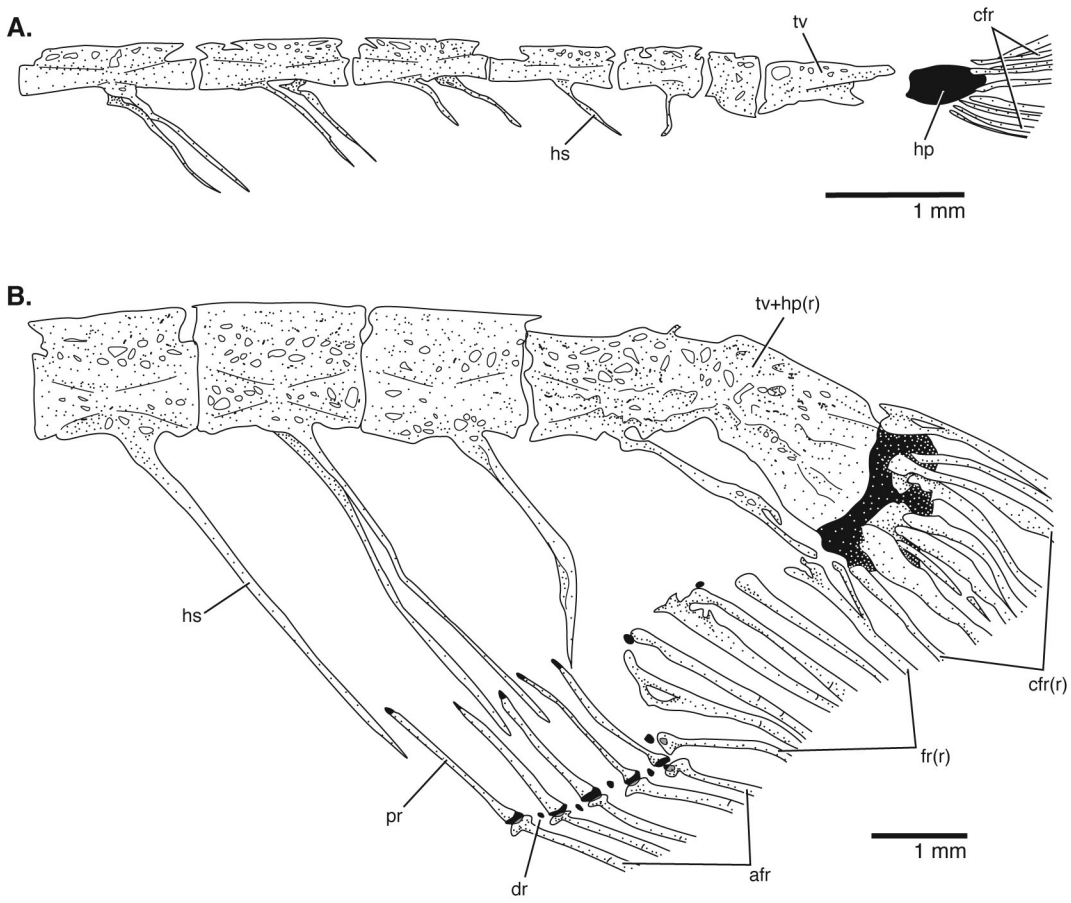

Fig. 17. Posteriormost caudal region showing (A) complete (FMNH 117281, 155 mm TL) and (B) regenerated conditions (ANSP 187028, 205 mm TL). Anterior facing left. Abbreviations: afr, anal fin ray; cfr, caudal fin ray; cfr(r), regenerated caudal fin ray; dr, distal radial; fr(r), regenerated fin ray; hp, hypural plate; hs, hemal spine; pr, proximal radial; tv, terminal vertebra; tv+hp(r), regenerated terminal vertebra and hypural plate.

The cleithrum is large, and is roughly shaped like a backwards L and supports a large, shallow fossa for the origin of the *m. sternohyoideus*. Anteriorly, the left and right cleithra contact each other in the ventral midline.

The chondral components of the pectoral girdle include the scapula, the mesocoracoid, and the coracoid (Fig. 18B). The scapula is broad, being visible laterally, and contacts the mesocoracoid anterodorsally and anteroventrally, and the coracoid ventrally. The mesocoracoid is an extremely thin strut of bone connecting the medial surface of the cleithrum with the dorsal margin of the scapula and coracoid. The coracoid is hook shaped, being broad dorsally and narrow anteroventrally where it tapers to a point. The supports for the pectoral fin include the propterygium, four pectoral radials, or actinosts (two supported by the scapula and two supported by the coracoid) and 11-13 distal radials.

Pelvic girdle and fin.— These elements are completely absent in *O. tamandua*, as in other Gymnotiformes (e.g., Fink and Fink, 1981; Mago-Leccia, 1994).

Scales.— The entire body except for the dorsal midline (the position of the dorsal filament) is covered by a dense array scales. Anteriorly on the body the scales are small and nearly circular whereas posteriorly they are larger and more rectangular with an angular posterior border (Fig. 19). All scales have a poorly mineralized focus and bear several circuli. The scale rows are numerous, and number about 12 above and 40 to 42 below the lateral line at the anterior portion of the caudal region (the exact number of scale rows was not possible to determine because they

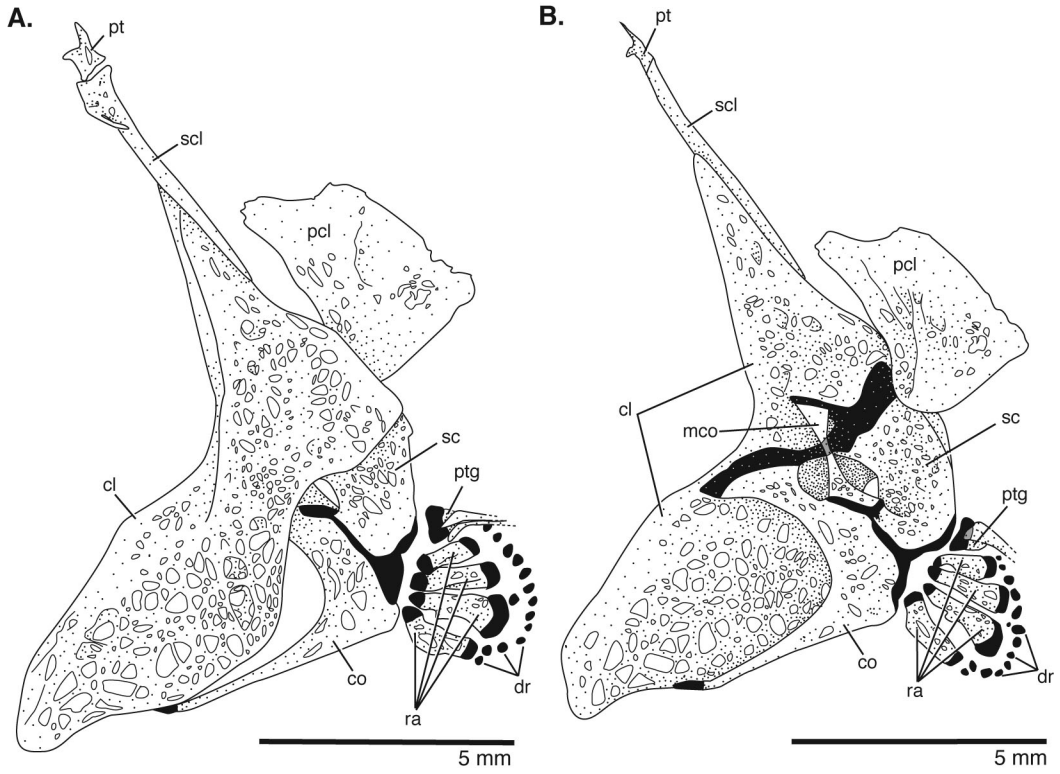

Fig. 18. Pectoral girdle of the right side in (A) lateral and (B) medial views; ANSP 187028, 205 mm TL. Anterior facing left (image in A reversed). Abbreviations: cl, cleithrum; co, coracoid; dr, distal radial; mco, mesocoracoid; pcl, postcleithrum; pt, posttemporal; ptg, propterygium; ra, radial; sc, scapula; scl, supracleithrum.

are loosely attached and are easily displaced – on not one of our cleared and stained specimens were we able to get an accurate count, and the scales on the alcohol specimens are equally difficult to get an accurate count from). The first five to ten scales along the lateral line are modified into strongly overlapping elongate tubes.

DISCUSSION

Electric organ discharges of Sternarchorhamphini.— To the best of our knowledge the EOD characteristics of *Orthosternarchus tamandua* have not been reported elsewhere. However, Bennett (1971) described the similar, though faster EODs of *Sternarchorhamphus muelleri* as "monophasic head-negative pulses superimposed on a fairly level head-positive base line with no dc component." Because our recordings of these gymnotiforms were AC-coupled we cannot ascertain where the waveforms cross the zero-potential line. However, as for the *S. muelleri* EOD, the positive and negative portions of the *O. tamandua* EOD are likely balanced such that no net direct current is produced. In his neurophysiological study of gymnotiform electric organs, Bennett (1971) examined the electric organ (EO) and EOD of *S. muelleri* and other apteronotids (although not that of *O. tamandua*) and presented a model for EOD waveform production based on the morphology of the individual electrocytes. In apteronotids these are spinal neurons rather than the modified muscle cells found in other gymnotiforms. Bennett (1971) discovered that in *S. muelleri* the electrocytes run in a caudal direction immediately upon entering the EO and lack the rostrally directed segment that produces the head-positive EOD spikes of other apteronotids. We have not examined the electric organ of *O. tamandua*, but given that its EOD is similar to that of *S. muelleri*, we suspect it shares this anatomical structure.

Interestingly, this monophasic waveform, seen only within these two genera among adult apteronotids, is very similar to that reported for a larval *Apteronotus* sp., which as an adult develops the typical biphasic EOD (Kirschbaum, 1983). Does then the EOD of *Sternarchorhamphus* and *Orthosternarchus* represent a derived paedomorphism or a primitive type of adult EOD for apteronotids (in which case the ontogenic stages observed in *Apteronotus* are seen to be a recapitulation of evolutionary history)? The phylogenetic hypothesis of Triques (2005) placing

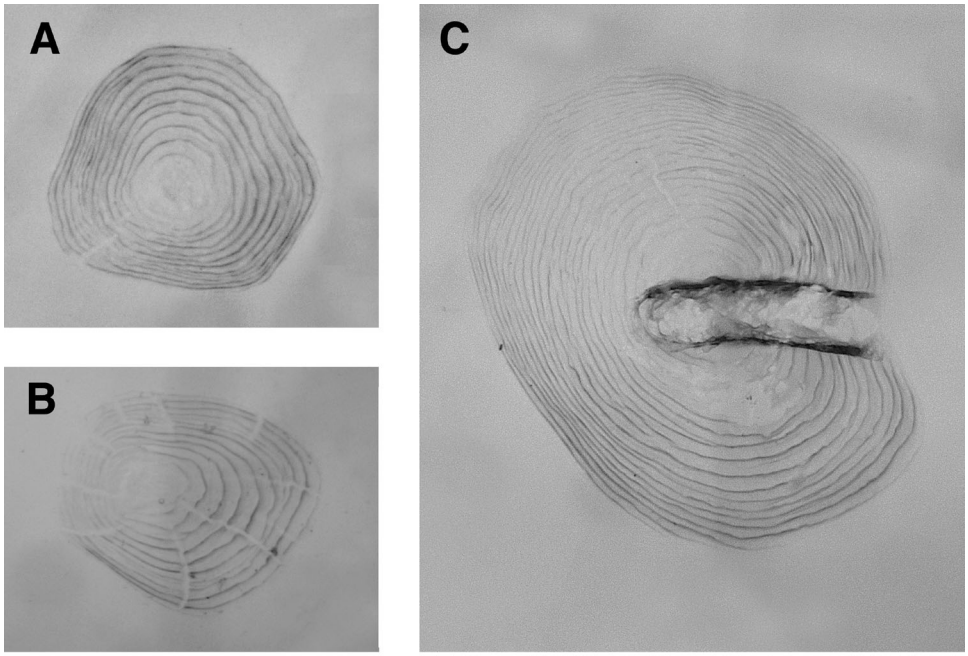

Fig. 19. Scales from (A) above and (B) below the lateral line, and (C) a lateral line scale from about half way down the caudal region from left side of cleared and stained specimen (FMNH 117281, 155 mm TL). Anterior facing left.

Orthosternarchus + *Sternarchorhamphus* as the sister group to the remaining apteronotids might permit the interpretation of their monophasic EOD as primitive relative to the biphasic EOD of other Apteronotidae. However this inference would also depend upon the phylogenetic position of Apteronotidae with respect to the other gymnotiform family groups as well as one's willingness to consider EOD monophasy and biphasy homologous character states across gymnotiform families, despite great differences in electrocyte structure. Given the phylogenetic and analytical uncertainties, we regard the evolutionary polarity of this character unresolved for the time being.

Phylogenetic affinities.— The interrelationships of genera within Apteronotidae are still the subject of debate (cf. results of Albert, 2001 and Triques, 2005) and are beyond the scope of this paper. However, we do take this opportunity to discuss the phylogenetic characters used in the past to place *Orthosternarchus*. One of the common relationships within the family Apteronotidae found in most studies, dating back to the work of Ellis (1913: plate 15), is the close (i.e., sister-group) relationship of *Orthosternarchus* and *Sternarchorhamphus* (= Sternarchorhamphini of Albert, 2001; Sternarchorhamphinae of Triques, 2005; in his textual description of various clades resulting from his phylogenetic analysis, Triques (2005) inexplicably used the name Orthosternarchinae in reference to the clade including *Orthosternarchus* and *Sternarchorhamphus*, although in both his abstract and concluding classification, he referred to this clade as "Sternarchorhamphinae Albert 2001 stat. n.," thereby elevating Albert's tribe Sternarchorhamphini to subfamily status).

Campos-da-Paz (1995) discussed numerous similarities between *Sternarchorhamphus* and *Orthosternarchus*, although he noted that there was insufficient knowledge of the later to firmly determine their relationship to one another. Alves-Gomes et al. (1995) found strong support for this group in their analysis of mitochondrial genetic data (99-100 bootstrap values). Albert (2001: 73) reported 12 unambiguous synapomorphies supporting these two genera as sister taxa, including: 1) absence of scales on the dorsal midline of body; 2) an elongate premaxilla; 3) two or three rows of teeth on the dentary; 4) the anterior part of the frontal concave; 5) the first infraorbital removed from the anterior infraorbital pore; 6) tiny eye with no extrinsic muscles; 7) ossified mesocoracoid present; 8) dorsal filament extending from back of skull to caudal peduncle; 9) anterior anal fin rays unbranched; 10) anal fin radials "arrow-head" shaped; 11) slender posterior parapophyses; and 12) monophasic depolarization of EODs. Triques (2005) listed two homoplasous characters (absence of ascending process of metapterygoid (= endopterygoid process), found also in certain species of *Apteronotus*, *Sternarchogiton*, and *Sternarchorhynchus*; and a single hemal spine located posterior to the posteroventral abdominal bone, found also in *Magosternarchus raptor* in his study) and three unambiguous characters in support of these two species as sister taxa, only one of which overlapped with Albert's synapomorphies: 1) snout very elongate, straight; 2) presence of less than 10 fin rays on the caudal fin; and 3) mesocoracoid present. Of these published data, we comment on Albert's characters 1 and 8, which may be correlated

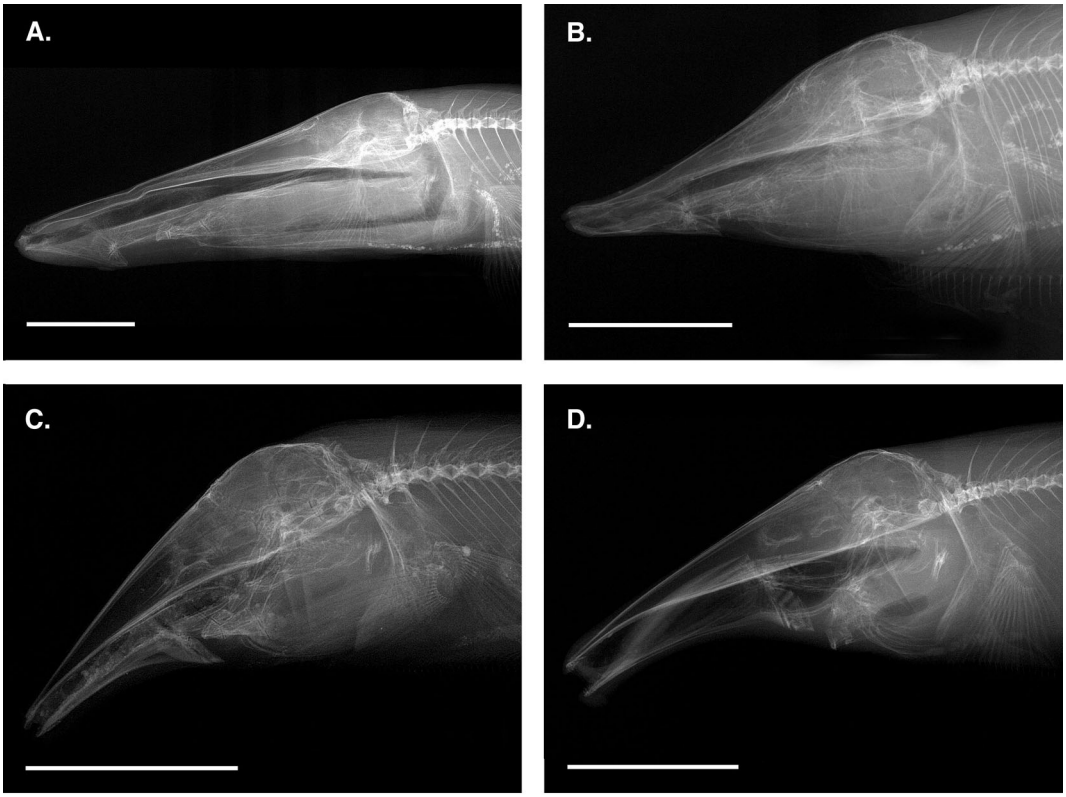

Fig. 20. Radiographs of heads and pectoral girdles of some long-snouted apteronotids (= Sternarchorhynchinae *sensu* Albert, 2001) in lateral view. (A) *Orthosternarchus tamandua* (USNM 375476). (B) *Sternarchorhamphus muelleri* (USNM 373235). (C) *Platyurosternarchus macrostomus* (USNM 305546). (D) *Sternarchorhynchus mormyrus* (USNM 306843). Scale bar equals 10 mm. Anterior facing left.

in that scales are typically absent from the surface of the dorsal filament in apteronotids (pers. obs.), and therefore the absence of scales from the entire dorsal midline of the body in *Orthosternarchus* is likely related to the continuation of the dorsal filament far anteriorly. Additionally, the coding of Triques' (2005) second homoplasy, concerning the number of hemal spines posterior to the posterior abdominal bone, is difficult to understand, as Albert (2001: fig. 36) clearly shows a condition similar to that in *Orthosternarchus* (see Fig. 16) in several other apteronotids, and codes it as such in his data matrix for most apteronotid genera and *Rhabdolichops*. Therefore, we cannot see this as support for *Orthosternarchus* + *Sternarchorhamphus*.

As shown above, the grouping *Orthosternarchus* + *Sternarchorhamphus* has received strong support from both morphological and molecular data. The phylogenetic affinities of these two genera within Apteronotidae, in contrast, remain unclear. These two genera were considered to be the sister-group to Sternarchorhynchini (= *Platyurosternarchus* + *Sternarchorhynchus*) by Albert (2001), forming his Sternarchorhynchinae (= Sternarchorhamphini + Sternarchorhynchini). An elongate preorbital region was one of the characters used by Albert (2001) in support of the Sternarchorhynchinae, as well as some related characters, such as an elongate ventral ethmoid. As he noted (p. 82), the elongation in all members of this subfamily involves both the orbital and ethmoidal regions. However, the way in which this elongation is reflected in the skeleton is very different in the two tribes. For instance, the lower jaw joint is relatively far back on the skull in *Platyurosternarchus* and *Sternarchorhynchus*, positioned roughly under the eye (Fig. 20). As a result, the lower jaws of these two genera are very elongate, spanning most of the preorbital region (Campos-da-Paz, 2000: fig. 6; see also Triques, 2005: figs. 17, 19). This is the reminiscent of the condition seen in other apteronotids with elongate snouts (e.g., male *Parapteronotus hasemani*; see Catania, 2002: 18). Conversely, in *Sternarchorhamphus* and *Orthosternarchus* the lower jaw joint is positioned more anteriorly on the snout and the lower jaw is not exceptionally elongate (Fig. 20; also Campos-da-Paz, 1995: figs. 4, 5 for *Sternarchorhamphus*). Therefore, the elongation of the head in the two groups is achieved in two very different manners. This independence was suggested by Triques (2005) as well, who found the group *Orthosternarchus* + *Sternarchorhamphus* to be the sister-group of all other

apteronotids, and far removed from other long-snouted apteronotids such as Sternarchorhynchini. See further discussion of elongation in the snout in Gymnotiformes by Albert (2001: 82), who concluded that this phenomenon of head elongation "evolved independently in Rhamphichthyidae and in at least three separate apteronotid lineages" (Sternarchorhynchinae, *Apteronotus brasiliensis* species-group, and *Parapteronotus* and *Compsaria*) and by Triques (2005), who concluded that elongation of the snout occurs independently in Sternarchorhynchini, *Orthosternarchus*, and *Sternarchorhamphus*. Undoubtedly multiple occurrences of a similar overall shape has occurred, and there has been much attention paid to it in recent cladistic analyses, yet there remains more to understand and discover about the taxonomic distribution and anatomical manifestations (i.e., sorting of homologous conditions) of the "snout elongation phenomenon" within gymnotiform fishes.

We conclude by noting that in either phylogenetic hypotheses of the two most recent phylogenetic studies (i.e., Albert's or Triques'), the group containing *Orthosternarchus* + *Sternarchorhamphus* (i.e., as a group in and of itself or as sister-group to *Sternarchorhynchus* + *Platyurosternarchus*) is relatively basal to all other apteronotid taxa, suggesting that this lineage split prior to most of the diversification of the family Apteronotidae. This topology is consistent also with the results of Alves-Gomes' et al. (1995) molecular study, although there was less resolution at the base of the family in this study.

ACKNOWLEDGEMENTS

For access to specimens in their care and other museum assistance, we thank J. Maclaine and P. Campbell (NHM), L. Rapp Py-Daniel (INPA), M. Westneat, M. A. Rogers, and K. Swagel (FMNH), K. Hartel (MCZ), G. D. Johnson, L. R. Parenti, R. Vari, J. Williams, L. Palmer and S. Smith (USNM). We thank S. Raredon (USNM) for assistance with the x-raying of specimens. B. Lehner, at the Conservation Science Program, World Wildlife Fund US, generously provided the base map used in Fig. 4. We thank R. Britz (NHM) for his constructive review of this manuscript and insightful discussions on the anatomy of fishes.

During a portion of this study, EJH was supported by a Smithsonian Fellowship at the USNM, and he is grateful for the opportunities this allowed him; his support by U.S. National Science Foundation (NSF) DEB-0414552 (to EJH and L. Grande) is also gratefully acknowledged.

The "Calhamazon Project" was supported by NSF DEB-9300151 (to JGL), the Office of Forestry, Environment and Natural Resources, Bureau of Science and Technology, of the U.S. Agency for International Development and the Conselho Nacional de Desenvolvimento Científico e Tecnológico (CNPq, Brazilian National Research Council). Permission to conduct research and collect in Brazil was granted by CNPq.

LITERATURE CITED

Albert, J. S. 2001. Species diversity and phylogenetic systematics of American knifefishes (Gymnotiformes, Teleostei). Miscellaneous Publications of the Museum of Zoology, University of Michigan 190: 1-127.

Albert, J. S. 2003. Family Apteronotidae (Ghost knifefishes). *In* S. Kullander, R. Reis and C. Ferraris (eds.). Check List of Freshwater Fishes of South and Central America. EDIPURCRS, Porto Alegre, pp. 504-509

Albert, J. S., and R. Campos-da-Paz. 1998. Phylogenetic systematics of Gymnotiformes with a diagnosis of 58 clades: a review of available data. *In* L. R. Malabarba, R. E. Reis, R. P. Vari, Z. M. S. Lucena and C. A. S. Lucena (eds.). Phylogeny and Classification of Neotropical Fishes. EDIPURCRS, Porto Alegre, pp. 419-446.

Alves-Gomes, J. A. 1999. Systematic biology of gymnotiform and mormyriform electric fishes: phylogenetic relationships, molecular clocks and rates of evolution in the mitochondrial rRNA genes. Journal of Experimental Biology 202: 1167-1183.

Alves-Gomes, J. A., G. Ortí, M. Haygood, W. Heiligenberg, and A. Meyer. 1995. Phylogenetic analysis of the South American electric fishes (Order Gymnotiformes) and the evolution of their electrogeneic system: a synthesis based on morphology, electrophysiology, and mitochondrial sequence data. Molecular Biology and Evolution 12: 298-318.

Barletta, M. 1995. Estudo da comunidade de peixes bentônicos em três areas do canal principal próximas a confluência dos rios Negro e Solimões – Amazonas (Amazônia Central – Brasil). Master's Thesis, INPA/UA, 114 pp.

Bennett, M. V. L. 1971. Electric organs. *In* W. S. Hoar and D. J. Randall (eds.). Fish Physiology. Academic Press, New York, pp. 347-491.

Boulenger, G. A. 1898. On a collection of fishes from the Rio Jurua, Brazil. Transactions of the Zoological Society of London 14: 421-428.

Britz, R., and M. Hoffmann. 2006. Ontogeny and homology of the claustra in otophysan Ostariophysi (Teleostei). Journal of Morphology 267: 909-923.

Campos-da-Paz, R. 1995. Revision of the South American freshwater fish genus *Sternarchorhamphus* Eigenmann, 1905 (Ostariophysi: Gymnotiformes: Apteronotidae), with notes on its relationships. Proceedings of the Biological Society of Washington 108: 29-44.

Catania, D. 2002. X-Ray Ichthyology: The Structure of Fishes. California Academy of Sciences, San Francisco.

Cox Fernandes, C. 1998. Sex-related morphological variation in two species of apteronotid fishes (Gymnotiformes) from the Amazon River Basin. Copeia 1998: 730-735.

Cox Fernandes, C. 1999. Detrended canonical correspondence analysis (DCCA) of electric fish assemblages in the Amazon. *In* A. Val and V. M. F. Almeida-Val (eds). Biology of Tropical Fishes. INPA, Manaus, pp. 21-39.

Cox Fernandes, C., J. G. Lundberg, and C. Riginos. 2002. Largest of all electric-fish snouts: hypermorphic facial growth in male *Apteronotus hasemani* and the identity of *Apteronotus anas*

(Gymnotiformes: Apteronotidae). Copeia 2002: 52-61.

Cox Fernandes, C., J. Podos, and J. G. Lundberg. 2004. Amazonian ecology: tributaries enhance the diversity of electric fishes. Science 305: 1960-1962.

Dingerkus, G., and L. D. Uhler. 1977. Enzyme clearing of alcian blue stained whole small vertebrates for demonstration of cartilage. Journal of Stain Technology 52: 229-232.

Eigenmann, C. H., and D. P. Ward. 1905. The Gymnotidae. Proceedings of the Washington Academy of Science 7: 157-186.

Eigenmann, C. H., and W. R. Allen. 1942. Fishes of Western South America. I. The Intercordilleran and Amazonian lowlands of Peru II. The High Pampas of Peru, Bolivia, and northern Chile, with a revision of the Peruvian Gymnotidae, and of the genus *Orestias*. The University of Kentucky, Lexington.

Ellis, M. M. 1913. The gymnotid eels of tropical America. Memoirs of the Carnegie Museum 6: 109-204.

Ferreira, A. B. de H. 1986. Editora Nova Fronteira S. A. Rio de Janeiro, RJ, Brazil.

Fink, S. L. and W. L. Fink. 1981. Interrelationships of the ostariophysan fishes (Teleostei). Zoological Journal of the Linnean Society 72: 297-353.

Franchina, C. R and C. D. Hopkins. 1996. The dorsal filament of the weakly electric Apteronotidae (Gymnotiformes; Teleostei) is specialized for electroreception. Brain Behavior and Evolution 47: 165-178.

Garcia, M. 1995. Aspectos ecológicos dos peixes das águas abertas de um lago no arquipélago das Anavilhanas, Rio Negro, AM. Master's Thesis, INPA/UA, 95 pp.

Hoffmann, M. and R. Britz. 2006. Ontogeny and homology of the neural complex of otophysan Ostariophysi. Zoological Journal of the Linnean Society 147: 301-330.

Jaeger, E. C. 1978. A Source-Book of Biological Names and Terms, Third Edition, Sixth Printing. Charles C. Thomas, Springfield, Illinois.

Jordan, D. S. 1923. A classification of fishes including families and genera as far as known. Stanford University Publications, University Series, Biological Sciences 3: 77-243.

Kirschbaum, F. 1983. Myogenic organ precedes the neurogenic organ in apteronotid fish. Naturwissenschaften 70: 205-207.

Leviton, A. E., R. H. Gibbs, Jr., E. Heal, and C. E. Dawson. 1985. Standards in herpetology and ichthyology: part I. Standard symbolic codes for institutional resource collections in herpetology and ichthyology. Copeia 1985: 802–832.

Lundberg, J. G., and F. Mago-Leccia. 1986. A review of *Rhabdolichops* (Gymnotiformes, Sternopygidae), a genus of South American freshwater fishes, with descriptions of four new species. Proceedings of the Academy of Natural Sciences of Philadelphia 138: 53-85.

Lundberg, J. G., C. Cox Fernandes, J. P. Albert, and M. Garcia. 1996. *Magosternarchus*, a new genus with two new species of electric fishes (Gymnotifirmes: Apteronotidae) from the Amazon river basin, South America. Copeia 1996: 657-670.

Mago-Leccia, F. 1994. Electric fishes of the continental waters of America. Fundacion para el desarrollo de las Ciencias Fisicas, Matematicas y Naturales, Caracas.

Moller, A. P., and J. P. Swaddle. 1997. Asymmetry, Developmental Stability, and Evolution. Oxford University Press, New York, 287 pp.

Northcutt, R. G. 1989. The phylogenetic distribution and innervation of craniate mechanoreceptive lateral lines. *In* S. Coombs, P. Gˆrner, and H. M¸nz (eds.). The Mechanosensory Lateral Line: Neurobiology and Evolution. Springer, New York, pp. 17-78

Palmer, A. R. and C. Strobeck. 1986. Fluctuating asymmetry: measurement, analysis, patterns. Annual Review of Ecology and Systematics, 17: 391-421.

Patterson, C., and G. D. Johnson. 1995. The intermuscular bones and ligaments of teleostean fishes. Smithsonian Contributions to Zoology, 559: 1-83.

Sioli, H. 1975. Amazon tributaries and drainage basins. In: Coupling of Land and Water Systems, A. D. Hasler (ed). Springer Verlag. New York: 199-213.

Thomé de Souza, M. J. F. 1999. Variação temporal e especial da comunidade de peixes bentônicos no baixo rio Branco e sua confluência com o rio Negro, durante uma estação forte e prolongada seca (El Ninõ 1997-98) (Bacia do rio Branco – Amazônia – Brasil). Master's Thesis, INPA/UA, 74 pp.

Triques, M. L. 1993. Filogenia dos gêneros de Gymnotiformes (Actinopterygii, Ostariophysi), com base em caracterers esqueléticos. Comunicacoes do Museu de Ciencias e Tecnologia da PUCRS. Serie Zoologia 6: 85-130.

Triques, M. L. 2005. Análise cladística dos caracteres de anatomia externa e esquelética de Apteronotidae (Teleostei: Gymnotiformes). Lundiana 6: 121-149.

APPENDIX 1: SPECIMENS EXAMINED

All specimens are alcohol-preserved s unless otherwise indicated. Most specimens were also x-rayed. Four specimens were cleared and double stained are ANSP 187034 (215 mm TL), FMNH 117281 (155 mm TL), ANSP 187028 (205 mm TL), and JNB 93-10 (uncatalogued; 235 mm TL).

Orthosternarchus tamandua
Rio Negro, Brazil: ANSP 187029 (1 male), ANSP 187030 (1 male), ANSP 187031 (1), ANSP 187032 (1), ANSP 187033 (1 juvenile), ANSP 187034 (1 female), ANSP 187037 (2 females), ANSP 187038 (1 male), FMNH 114910 (1), FMNH 114911 (1), FMNH 114912 (3), FMNH 114913 (2), FMNH 114914 (1), FMNH 114915 (1), FMNH 114917 (1), MCZ 98368 (1), USNM 373017 (3), USNM 373033 (2), USNM 373071 (1), USNM 373072 (2), USNM 375476 (4, 1 of them a female), USNM 375477 (1 female, 2 males), FMNH 117281 (1), JNB 93.10 (uncatalogued; 1 female). Rio Branco, Brazil: FMNH 114908 (1), FMNH 114909 (1), USNM 373072 (2), USNM 373035 (1). Rio Içа, Brazil: ANSP 187036 (1 male), ANSP 187043 (1 juvenile), ANSP 187044 (1 female). Rio Jutaí, Brazil: ANSP 187041 (1 female), JGL 69-93 (uncatalogued; 1 juvenile). Rio Juruá, Brazil: OTO 23/2 (uncatalogued; 1). Rio Purus, Brazil: ANSP 187025 (1 male), ANSP 187039 (1 male), ANSP 187040 (2), ANSP 187045 (1 male), ANSP 187046 (1 male), ANSP 187047 (1 male), INPA 15011 (2). Rio Pará, Brazil: ANSP 187021 (2 females), ANSP 187022 (1). Rio Jari, Brazil: ANSP 187024 (1 female). Rio Trombetas, Brazil: ANSP 187035 (1 female). Rio Solimões, Brazil: ANSP 187028 (1 female). Rio Amazonas, Brazil: ANSP 187023 (1 male), ANSP 187026 (1 male, 1 female), ANSP 187027 (1 female, 1 male), FMNH 114916 (1), INPA 15012 (2), INPA 15013 (3), INPA 15014 (1). Parana do Mamia, Brazil: ANSP 187042 (1 female).Furus (channels) above Pará, Brazil: ANSP 187018 (1 female), ANSP 187017 (1 male), ANSP 187019 (1 female), ANSP 187020 (1 male). Rio Jaú, Brazil: INPA 12632 (1), INPA 12621 (1).

Platyurosternarchus macrostomus
Rio Matos, Bolivia: USNM 305546 (2)

Sternarchorhamphus muelleri
Rio Negro, Brazil: USNM 373235 (1)

Sternarchorhynchus mormyrus
Ressaca de Ilha de Marchantaria, Brazil: USNM 306843 (2)

Table 1. Summary of body measurements for a sample of *Orthosternarchus tamandua* (n=47 for all variables except AFL, for which n=32).

	Total Length (TL)	Body Length to 100th AnalFin Ray (L100)	Anal Fin Length (AFL)	Pre-Dorsal Thong Length (LOD)	Depth of Abdominal Cavity (AB)	Maximum Body Depth (BD)
Range	97.7-450.0	66.6-249.0	92.5-391.0	15.5-91.9	10.0-37.2	11.2-45.2
(as % L100)	(—)	(—)	(127.2-196.1)	(23.3-47.9)	(14.6-21.4)	(16.5-25.7)
Mean	274.8	146.0	227.2	59.8	25.3	30.9

Table 2. Summary of head measurements for a sample of *Orthosternarchus tamandua* (n=47 for all variables).

	Head Length (H)	Head Depth (HD)	Pre-nares Length (N)	Internarial Distance (ID)	Mouth Length (M)
Range	16.9-81.5	7.9-32.2	1.4-4.0	1.6-4.3	1.8-7.8
(as % L100)	(25.4-43.9)	(11.3-17.7)	(1.4-2.3)	(1.3-2.8)	(2.7-5.1)
Mean	54.2	19.8	2.7	2.8	5.6